Nuclear charge-exchange excitations based on a relativistic density-dependent point-coupling model

Vale, D.; Niu, Y. F.; Paar, N.

Nuclear charge-exchange excitations based on a relativistic density-dependent point-coupling model

D. Vale [*]
Gimnazija i strukovna škola Jurja Dobrile Pazin, Šetalište Pazinske gimnazije 11, Pazin 52000, Croatia; Osnovna škola Vodnjan/Scuola elementare Dignano, Žuka 6/Via delle ginestre 6, Vodnjan/Dignano 52215, Croatia; and Department of Physics, Faculty of Science, University of Zagreb, Bijenička cesta 32, 10000 Zagreb, Croatia

Y. F. Niu
School of Nuclear Science and Technology, Lanzhou University, Lanzhou 730000, China and ELI-NP, Horia Hulubei National Institute for Physics and Nuclear Engineering, 30 Reactorului Street, RO-077125, Bucharest-Magurele, Romania

N. Paar [†]
Department of Physics, Faculty of Science, University of Zagreb, Bijenička cesta 32, 10000 Zagreb, Croatia

(Received 18 December 2020; revised 21 April 2021; accepted 26 May 2021; published 8 June 2021)

Spin-isospin transitions in nuclei away from the valley of stability are essential for the description of astrophysically relevant weak interaction processes. While they remain mainly beyond the reach of experiment, theoretical modeling provides important insight into their properties. In order to describe the spin-isospin response, the proton-neutron relativistic quasiparticle random phase approximation is formulated using the relativistic density-dependent point coupling interaction, and separable pairing interaction in both the $T = 1$ and $T = 0$ pairing channels. By implementing recently established DD-PCX interaction with improved isovector properties relevant for the description of nuclei with neutron-to-proton number asymmetry, the isobaric analog resonances (IAR) and Gamow-Teller resonances (GTR) have been investigated. In contrast to other models that usually underestimate the IAR excitation energies in Sn isotope chain, the present model accurately reproduces the experimental data, while the GTR properties depend on the isoscalar pairing interaction strength. This framework provides not only an improved description of the spin-isospin response in nuclei, but it also allows future large-scale calculations of charge-exchange excitations and weak interaction processes in stellar environment.

DOI: 10.1103/PhysRevC.103.064307

I. INTRODUCTION

Charge-exchange excitations in atomic nuclei correspond to a class of nuclear transitions composed of the particle-hole configurations that contain the exchange of the nucleon charge, described by the isospin projection lowering (increasing) operator τ_- (τ_+). The fundamental charge-exchange excitation is the isobaric analog resonance (IAR) [1–8], with no changes in quantum numbers $\Delta J = \Delta L = \Delta S = 0$, thus the IAR corresponds to a collective excitation with $J^\pi = 0^+$. The Gamow-Teller resonance (GTR) represents another relevant charge-exchange mode, characterized by $J^\pi = 1^+$, i.e., it corresponds to spin-flip excitations without changing the orbital motion, $\Delta S = 1$, $\Delta L = 0$.

As it has been emphasized in Ref. [9], recent interest in the GTR studies is motivated by its importance for understanding the spin and spin-isospin dependence of modern effective interactions [10–17], nuclear β decay [18–26], β-delayed neutron emission [27], as well as double β decay [28–36]. In addition, accurate description of GT$^\pm$ transitions, including both in stable and exotic nuclei, is relevant for the description of a variety of astrophysically relevant weak interaction processes [37–41], electron capture in presupernova stars [42–44], r-process [45,46] and neutrino-nucleus interaction of relevance for neutrino detectors and neutrino nucleosynthesis in stellar environment [47–53].

The properties of charge-exchange modes of excitation have extensively been studied [54,55]. Following theoretical prediction [56], in 1975 the GTR has been experimentally confirmed in (p, n) reactions [57]. The GTR represents one of the most extensively investigated collective excitation in nuclear physics, both experimentally and theoretically (e.g., see Refs. [10,54,55,57–86]). More details about experimental studies of spin-isospin excitations are also reviewed in Ref. [55]. Recent studies of the GTR in the framework based on relativistic energy density-functional include relativistic quasiparticle random phase approximation (RQRPA) [6], the relativistic RPA based on the relativistic Hartree-Fock (RHF) [87], relativistic QRPA based on point coupling model with nonlinear interactions [25,43], and relativistic QRPA formulated using the relativistic Hatree-Fock-Bogoliubov (RHFB) model for the ground state [88]. In Ref. [89] the nuclear density-functional framework, based on chiral dynamics and the symmetry breaking pattern of low-energy

[*] deni.vale1@skole.hr
[†] npaar@phy.hr

QCD, has been used to formulate the proton-neutron QRPA to investigate the role of chiral pion-nucleon dynamics in the description of charge-exchange excitations. The GTR has also been studied by including couplings between single nucleon and collective nuclear vibrations, e.g., particle-vibration coupling (PVC) of the 1p-1h $\otimes$ phonon type of coupling [79,84,90,91]. The PVC allows to include important dynamical correlations missing in the static self-consistent mean field models and it provides additional fragmentation of the GTR strength when compared to the random phase approximation studies based only on 1p-1h configurations [79].

At present, the knowledge about charge-exchange transitions in nuclei away from the valley of stability is rather limited, and mainly beyond the reach of experiment. Since these nuclei are especially important for their astrophysical relevance in stellar evolution and nucleosynthesis, it is crucial to develop microscopic theoretical approaches, that allow quantitative and systematic analyses of the transition strength distributions of unstable nuclei. In order to assess the overview into systematical model uncertainties in modeling charge-exchange excitation phenomena, it is important to address their properties from various approaches, by implementing different theory frameworks and effective nuclear interactions.

In Ref. [6] charge-exchange excitations have been studied in the framework based on the relativistic nuclear energy density-functional (EDF), within the approach that unifies the treatment of mean-field and pairing correlations, relativistic quasiparticle random phase approximation (RQRPA) formulated in the canonical single-nucleon basis of the relativistic Hartree-Bogoliubov (RHB) model. In this implementation the relativistic EDF with explicit density dependence of the meson-nucleon couplings is used, that provides an improved description of asymmetric nuclear matter, neutron matter and nuclei far from stability. The pairing correlations were described by the pairing part of the finite range Gogny interaction [92,93]. However, the EDFs have usually been parameterized with the experimental data on the ground-state properties, supplemented with the pseudo-observables on nuclear matter properties. In the case of density-dependent meson-exchange interactions, the neutron skin thickness in ^{208}Pb has been introduced as an additional constraint on the isovector channel of the effective interaction. However, the results from measurements of the neutron-skin thickness are usually model dependent, and the pseudo-observables on nuclear matter are often rather arbitrary. Recently, a novel EDF parametrization has been established based on the relativistic point coupling interaction, by using in the χ^2 minimization the nuclear ground-state properties (binding energies, charge radii, pairing gaps) together with the properties of collective excitations in nuclei, isoscalar giant monopole resonance energy and dipole polarizability [94]. In this way an effective interaction DD-PCX has been established with improved isovector properties, that is successful not only in the description of nuclear ground state, but also of the excitation phenomena, incompressibility of nuclear matter and the symmetry energy close to the saturation density [94]. The improved isovector channel for the DD-PCX interaction is especially important not only for the symmetry energy of the nuclear equation of state, but also for the description of ground-state and excitation properties of $N \neq Z$ nuclei. Clearly, this is very important for the implementation of the EDF-based models to exotic nuclei, as well as for applications in nuclear astrophysics.

In this work we establish the proton-neutron RQRPA in the canonical single-nucleon basis of the RHB model based on density-dependent relativistic point coupling interaction. Our study represents the first implementation of the relativistic point coupling interaction with density-dependent vertex functions in formulating the RQRPA for the description of charge-exchange excitations. In addition, the treatment of the pairing correlations is also improved, by implementing the separable pairing force that allows accurate and efficient calculations of the pairing properties [95]. By using recently established DD-PCX interaction with improved properties that are essential for description of nuclei away from the valley of stability [94], the proton-neutron RQRPA established in this work will be employed in the investigation of the properties of collective charge-exchange excitations, IAR and GTR.

Clearly, a study of both the IAR and GTR properties represents an important benchmark test for novel theoretical approaches established not only for description of charge-excitation modes but also for modeling a variety of astrophysically relevant processes in stellar environment. Therefore, in the present work that introduces a microscopic approach to describe charge-exchange excitations based on density-dependent relativistic point coupling interaction, the novel theory framework will be employed in the analyses of charge-exchange modes, the IAR and GTR, both for magic nuclei, as well as for open-shell nuclei to probe the effect of the pairing correlations.

In Sec. II the formalism of the proton-neutron RQRPA based on the density-dependent point coupling interaction is introduced. In Sec. III the model is employed in studies of charge-exchange modes of excitation, the IAR and the GTR. The conclusions of this work are summarized in Sec. IV.

II. PROTON-NEUTRON RQRPA BASED ON RELATIVISTIC POINT COUPLING INTERACTION

In the previous implementation in the relativistic framework, the RQRPA has been established on the ground of RHB model, based on the effective Lagrangian with density-dependent meson-exchange interaction terms [6]. Therein the pairing correlations have been described by the pairing part of the Gogny interaction [92,93]. In the present study, the RQRPA is established using the relativistic point coupling interaction, while the pairing correlations are described by the separable pairing force from Ref. [95]. Since the full RQRPA equations are rather complicated, in the present study we solve the respective equations in the canonical basis, where the Hartree-Bogoliubov wave functions can be expressed in the form of the BCS-like wave functions. More details on the implementation of the canonical basis in the RHB model and general formalism of the PN-RQRPA equations in the canonical basis are given in Ref. [6]. The focus of this work is the implementation of the relativistic point coupling

interaction in deriving the PN-RQRPA equations. The nuclear ground-state properties are described in the RHB model for the point coupling interaction, described in detail in Ref. [96].

Starting from the 0^+ ground state of a spherical even-even nucleus, transitions to J^π excited state of the corresponding odd-odd daughter nucleus are considered, using the charge-exchange operator $\mathcal{O}^{JM}$. The general form of the PN-RQRPA equations read [6],

$$\begin{pmatrix} A^J & B^J \\ B^{*J} & A^{*J} \end{pmatrix} \begin{pmatrix} X^{\lambda J} \\ Y^{\lambda J} \end{pmatrix} = E_\lambda \begin{pmatrix} 1 & 0 \\ 0 & -1 \end{pmatrix} \begin{pmatrix} X^{\lambda J} \\ Y^{\lambda J} \end{pmatrix}, \tag{1}$$

where the A and B matrices are defined in the canonical basis,

$$\begin{aligned} A^J_{pn,p'n'} &= H^{11}_{pp'}\delta_{nn'} + H^{11}_{nn'}\delta_{pp'} + (u_p v_n u_{p'} v_{n'} + v_p u_n v_{p'} u_{n'}) V^{phJ}_{pn'np'} + (u_p u_n u_{p'} u_{n'} + v_p v_n v_{p'} v_{n'}) V^{ppJ}_{pnp'n'} \\ B^J_{pn,p'n'} &= (u_p v_n v_{p'} u_{n'} + v_p u_n u_{p'} v_{n'}) V^{phJ}_{pn'np'} - (u_p u_n v_{p'} v_{n'} + v_p v_n u_{p'} u_{n'}) V^{ppJ}_{pnp'n'}. \end{aligned} \tag{2}$$

The proton and neutron quasiparticle canonical states are denoted by p, $p\prime$, and n, $n\prime$, respectively. V^{ph} is the proton-neutron particle-hole residual interaction, and V^{pp} is the corresponding particle-particle interaction, and u and v denote the occupation amplitudes of the respective states. Since the canonical basis does not diagonalize the Dirac single-nucleon mean-field Hamiltonian, the off-diagonal matrix elements $H^{11}_{nn'}$ and $H^{11}_{pp'}$ are also included in the A matrix, as given in Ref. [6]. E_λ denote the excitation energy, while $X^{\lambda J}$ and $Y^{\lambda J}$ are the corresponding forward- and backward-going QRPA amplitudes, respectively.

By solving the eigenvalue problem (1), the reduced transition strength can be obtained between the ground state of the even-even (N, Z) nucleus and the excited state of the odd-odd $(N+1, Z-1)$ or $(N-1, Z+1)$ nucleus, using the corresponding transition operators $\mathcal{O}^{JM}$ in both channels,

$$B^-_{\lambda J} = \left| \sum_{pn} < p||\mathcal{O}^J||n > \left(X^{\lambda J}_{pn} u_p v_n + Y^{\lambda J}_{pn} v_p u_n\right) \right|^2, \tag{3}$$

$$B^+_{\lambda J} = \left| \sum_{pn} (-1)^{j_p + j_n + J} < n||\mathcal{O}^J||p > \left(X^{\lambda J}_{np} v_p u_n + Y^{\lambda J}_{np} u_p v_n\right) \right|^2. \tag{4}$$

For the presentation purposes, the discrete strength distribution is folded by the Lorentzian function of the width $\Gamma = 1$ MeV,

$$R(E)^\pm = \sum_\lambda B^\pm_{\lambda J} \frac{1}{\pi} \frac{\Gamma/2}{(E - E_{\lambda_\pm})^2 + (\Gamma/2)^2}. \tag{5}$$

In the implementation of the relativistic point coupling interaction, the spin-isospin-dependent terms in the residual interaction of the PN-RQRPA are induced by the isovector-vector and pseudovector terms. In comparison, for the finite range meson-exchange interaction, these terms were obtained from the ρ-and π-meson exchange, respectively [6]. In the present study, the PN-RQRPA residual interaction terms V_{abcd} are derived from the effective Lagrangian density for the point coupling interaction.

The isovector-vector part of PN-RQRPA contains only nonrearrangement terms of the residual two-body interaction. For the respective spacelike components we obtain,

$$V^{(\mathrm{TVs})}_{abcd} = -\int d^3 r_1 \int d^3 r_2 \psi^\dagger_a(\vec{r}_1)(\vec{\tau}\gamma_0\gamma_i)^{(1)}\psi_c(\vec{r}_1)\alpha_{\mathrm{TV}}(\rho)\delta(\vec{r}_1 - \vec{r}_2)\psi^\dagger_b(\vec{r}_2)\left(\vec{\tau}\gamma_0\gamma^i\right)^{(2)}\psi_d(\vec{r}_2), \tag{6}$$

and timelike components are given by

$$V^{(\mathrm{TVt})}_{abcd} = \int d^3 r_1 \int d^3 r_2 \psi^\dagger_a(\vec{r}_1)\vec{\tau}^{(1)}\psi_c(\vec{r}_1)\alpha_{\mathrm{TV}}(\rho)\delta(\vec{r}_1 - \vec{r}_2)\psi^\dagger_b(\vec{r}_2)\vec{\tau}^{(2)}\psi_d(\vec{r}_2), \tag{7}$$

where the coupling $\alpha_{\mathrm{TV}}(\rho)$ is a function of baryon (vector) density. For Dirac spinor given by,

$$\psi_{am_a}(r) = \begin{bmatrix} f_a(r)\Omega_{\kappa_a m_a}(\Omega) \\ i g_a(r)\Omega_{\bar{\kappa}_a m_a}(\Omega) \end{bmatrix}, \tag{8}$$

where a stands for all quantum numbers, with the exception of the projection of total angular momentum m_a. Quantum number κ is defined as $\kappa = -(l+1)$ for $j = l + 1/2$ and $\kappa = l$ for $j = l - 1/2$, while $\bar{l} = 2j - l$ corresponds to the lower component orbital angular momentum [97]. The spacelike part of the matrix elements obtained by the angular momentum coupling is given

$$\begin{aligned} V^{(\mathrm{TVs})J}_{abcd} = \frac{2}{(2J+1)} \sum_L \int dr r^2 \alpha_{\mathrm{TV}}(\rho) [f_a(r) g_c(r) \langle (1/2\ l_a) j_a || [\sigma_S Y_L]_J || (1/2\ \bar{l}_c) j_c \rangle - g_a(r) f_c(r) \langle (1/2\ \bar{l}_a) j_a || [\sigma_S Y_L]_J || (1/2\ l_c) j_c \rangle] \\ \times [f_b(r) g_d(r) \langle (1/2\ \bar{l}_d) j_d || [\sigma_S Y_L]_J || (1/2\ l_b) j_b \rangle - g_b(r) f_d(r) \langle (1/2\ l_d) j_d || [\sigma_S Y_L]_J || (1/2\ \bar{l}_b) j_b \rangle], \end{aligned} \tag{9}$$

and the timelike part is

$$V_{abcd}^{(\mathrm{TVt})J} = \frac{2}{2J+1}\int drr^2\alpha_{\mathrm{TV}}(\rho)[f_a(r)f_c(r)+g_a(r)g_c(r)][f_b(r)f_d(r)+g_b(r)g_d(r)] \times \langle(1/2\ l_a)j_a||Y_J||(1/2\ l_c)j_c\rangle\langle(1/2\ l_d)j_d||Y_J||(1/2\ l_b)j_b\rangle. \tag{10}$$

When compared to standard R(Q)RPA matrix elements, in particular corresponding direct term, there exists an additional factor of 2 in the numerator of Eqs. (9) and (10) due to the difference in the isospin part of the matrix element (see Appendix A). The isovector-pseudovector part of the point coupling interaction is given by

$$V_{\mathrm{PV}} = -\alpha_{\mathrm{PV}}\delta(\vec{r}_1-\vec{r}_2)(\gamma_0\gamma_5\gamma_\mu\vec{\tau})^{(1)}(\gamma_0\gamma_5\gamma^\mu\vec{\tau})^{(2)}, \tag{11}$$

where α_{PV} denotes the strength parameter of the interaction. Since α_{PV} remains a free parameter of the model that cannot be constrained by the ground-state properties, its value should be constrained by the experimental data on charge-exchange excitations. For the corresponding timelike part of the pseudovector matrix elements we obtain,

$$V_{abcd}^{\mathrm{PV(t)J}} = \frac{2\alpha_{\mathrm{PV}}}{2J+1}\int drr^2[f_a(r)g_c(r)-g_a(r)f_c(r)][f_b(r)g_d(r)-g_b(r)f_d(r)] \times \langle(1/2\ l_a)j_a||Y_J||(1/2\ \bar{l}_c)j_c\rangle\langle(1/2\ \bar{l}_d)j_d||Y_J||(1/2\ l_c)j_c\rangle. \tag{12}$$

We note that the timelike matrix elements are nonzero only in the case of unnatural parity transitions, e.g., for Gamow-Teller transitions. The spacelike part of the isovector-pseudovector matrix elements results,

$$\begin{aligned} V_{abcd}^{\mathrm{PV(s)}J} = \frac{2\alpha_{\mathrm{PV}}}{2J+1}\sum_L\int drr^2[&f_a(r)f_c(r)\langle(1/2\ l_a)j_a||[\sigma_S Y_L]_J||(1/2\ l_c)j_c\rangle \\ &+ g_a(r)g_c(r)\langle(1/2\ \bar{l}_a)j_a||[\sigma_S Y_L]_J||(1/2\ \bar{l}_c)j_c\rangle][f_b(r)f_d(r)\langle(1/2\ l_d)j_d||[\sigma_S Y_L]_J||(1/2\ l_b)j_b\rangle \\ &+ g_b(r)g_d(r)\langle(1/2\ \bar{l}_d)j_d||[\sigma_S Y_L]_J||(1/2\ \bar{l}_b)j_b\rangle]. \end{aligned} \tag{13}$$

In order to constrain the value of the pseudovector coupling α_{PV}, we follow the same procedure as used in the case of relativistic functionals with meson exchange [6], i.e., α_{PV} is adjusted to reproduce the experimental value of excitation energy for Gamow-Teller resonance in ^{208}Pb, $E = 19.2$ MeV [98–100]. In this way, we obtain $\alpha_{\mathrm{PV}} = 0.734$ for DD-PC1, and $\alpha_{\mathrm{PV}} = 0.621$ for DD-PCX point coupling interaction, and use these values systematically in all further investigations.

The PN-RQRPA also includes the pairing correlations. In most of the previous applications of the RHB+RQRPA model, the pairing correlations have been described by the paring part of the Gogny force D1S [92,93]. This interaction has already been used in the RHB calculations of various ground-state properties in nuclei [101]. Since the calculations based on the finite range Gogny force require considerable computational effort, in the present formulation of the PN-RQRPA the separable form of the pairing interaction is used [95]. In Ref. [95], Y. Tian *et al.* introduced separable pairing interaction in the gap equation of symmetric nuclear matter in $^1S_0$ channel:

$$\Delta(k) = -\int_0^\infty \frac{k'^2dk'}{2\pi^2}\langle k|V_{\mathrm{sep}}^{^1S_0}|k'\rangle\frac{\Delta(k')}{2E(k')}, \tag{14}$$

where

$$\langle k|V_{\mathrm{sep}}^{^1S_0}|k'\rangle = -G_0p(k)p(k'), \tag{15}$$

with Gaussian ansatz

$$p(k) = e^{-a^2k^2}. \tag{16}$$

The two parameters a and G_0 were adjusted to density dependence of the gap at the Fermi surface in nuclear matter, calculated with the Gogny force [95]. After transformation of the pairing force from momentum to coordinate space one obtains,

$$V(\vec{r}_1,\vec{r}_2,\vec{r}_1',\vec{r}_2') = -G_0\delta(\vec{R}_1-\vec{R}_2)G(r)G(r')\frac{1-\hat{P}^\sigma}{2}, \tag{17}$$

where $\vec{r} = 1/\sqrt{2}(\vec{r}_1-\vec{r}_2)$ and $\vec{R} = 1/\sqrt{2}(\vec{r}_1+\vec{r}_2)$. $G(r)$ is the Fourier transform of $p(k)$,

$$G(r) = \frac{e^{-r^2/(2a^2)}}{(4\pi a^2)^{3/2}}. \tag{18}$$

Thus, the pairing force has finite range, and due to the presence of the factor $\delta(\vec{R}_1-\vec{R}_2)$ it preserves the translational invariance [95]. Due to coordinate transformation from laboratory to center of mass system and relative coordinates we need to use

Talmi-Moschinsky brackets,

$$|n_1 l_1, n_2 l_2; \lambda\mu\rangle = \sum_{NLnl} M^{NLnl}_{n_1 l_1 n_2 l_2} |NL, nl; \lambda\mu\rangle. \tag{19}$$

The definition of $M^{NLnl}_{n_1 l_1 n_2 l_2}$ is given in Refs. [102,103]. If the transformation matrix between two laboratory coordinates $\vec{r}_1$ and $\vec{r}_2$, and center of mass $\vec{R}$ and relative coordinate $\vec{r}$ is given

$$\begin{pmatrix} \vec{R} \\ \vec{r} \end{pmatrix} = \begin{pmatrix} \sqrt{\frac{d}{1+d}} & \sqrt{\frac{1}{1+d}} \\ \sqrt{\frac{1}{1+d}} & -\sqrt{\frac{d}{1+d}} \end{pmatrix} \begin{pmatrix} \vec{r}_1 \\ \vec{r}_2 \end{pmatrix}, \tag{20}$$

as a function of transformation parameter d [103], then the most general definition of coefficient $M^{NLnl}_{n_1 l_1 n_2 l_2}$ is given by

$$\begin{aligned} M^{NLnl}_{n_1 l_1 n_2 l_2}(d) = {} & i^{-(l_1+l_2+L+l)} 2^{-(l_1+l_2+L+l)/4} \sqrt{n_1! n_2! N! n! [2(n_1+l_1)+1]!! [2(n_2+l_2)+1]!!} \\ & \times \sqrt{[2(N+L)+1]!! [2(n+l)+1]!!} \sum_{abcd l_a l_b l_c l_d} (-1)^{l_a+l_b+l_c} (-1)^{(l_a+l_b+l_c+l_d)/2} d^{(2a+l_a+2d+l_d)/2} \\ & \times \frac{[(2l_a+1)(2l_b+1)(2l_c+1)(2l_d+1)]}{a! b! c! d! [2(a+l_a)+1]!! [2(b+l_b)+1]!! [(2(c+l_c)+1]!! [2(d+l_d)+1]!!} \\ & \times (1+d)^{-(2a+l_a+2b+l_b+2c+l_c+2d+l_d)/2} \langle l_a 0 l_c 0 | L 0\rangle \langle l_b 0 l_d 0 | l 0\rangle \langle l_a 0 l_b 0 | l_1 0\rangle \langle l_c 0 l_d 0 | l_2 0\rangle \begin{Bmatrix} l_a & l_b & l_1 \\ l_c & l_d & l_2 \\ L & l & \Lambda \end{Bmatrix}. \end{aligned} \tag{21}$$

By employing the basis of spherical harmonic oscillator,

$$\tilde{I}_n = \sqrt{4\pi} \int R_{nl}(r) G(r) r^2 dr = \frac{1}{2^{2/3} \pi^{3/4} b^{3/2}} \frac{(1-\alpha^2)^n}{(1+\alpha^2)^{n+3/2}} \frac{\sqrt{2n+1}}{2^n n!}, \tag{22}$$

the coupled matrix element for $T = 1$ pairing is given by

$$V^{(\text{pair})JM}_{abcd} = -G_0 \hat{j}_a \hat{j}_b \hat{j}_c \hat{j}_d (-1)^{l_b+l_d+j_a+j_c} \begin{Bmatrix} l_a & j_a & 1/2 \\ j_b & l_b & J \end{Bmatrix} \begin{Bmatrix} l_c & j_c & 1/2 \\ j_d & l_d & J \end{Bmatrix} \sum_{Nnn'} \tilde{I}_n \tilde{I}_{n'} M^{NJn0}_{n_a l_a n_b l_b} M^{NJn'0}_{n_c l_c n_d l_d}. \tag{23}$$

Furthermore, for Gamow-Teller transitions in open-shell nuclei we need to extend Eq. (23) to include both $T = 0$ and $T = 1$ channels. Therefore, we introduce natural extension of the pairing:

$$V^{(\text{pair})JM}_{abcd} = -G_0 \hat{j}_a \hat{j}_b \hat{j}_c \hat{j}_d \sum_{LS} \sum_{T} \frac{1}{2} [1 + (-1)^{S'+T+1}] \tilde{f}(S,T) \hat{S}^2 \hat{L}^2 \begin{Bmatrix} l_b & 1/2 & j_b \\ l_a & 1/2 & j_a \\ L & S & J \end{Bmatrix} \begin{Bmatrix} l_d & 1/2 & j_d \\ l_c & 1/2 & j_c \\ L & S & J \end{Bmatrix} \sum_{nn'} \tilde{I}_n \tilde{I}'_n M^{NLn0}_{n_a l_a n_b l_b} M^{NLn'0}_{n_c l_c n_d l_d}. \tag{24}$$

This is nonvanishing only for $S = 0$ and $T = 1$ or $S = 1$ and $T = 0$ pairing. Therefore, $\tilde{f}(S = 0, T = 1) = 1$ case corresponds to the Eq. (23), while the case $\tilde{f}(S = 1, T = 0) = V_{0pp}$. See Appendix B for detailed derivation. We do not know *a priori* the value of the isoscalar proton-neutron pairing strength parameter V_{0pp}. It may be somewhat reduced or enhanced compared to the case $T = 1(S = 0)$, which is only present at the RHB level, and should be deduced from experimental data on excitations or charge-exchange processes in open-shell nuclei.

In comparison to the nuclear ground state based on the RHB, the PN-RQRPA residual interaction includes an additional channel, described by the pseudovector term and additional $T = 0$ $(S = 1)$ pairing term for Gamow-Teller transitions in open-shell nuclei, that are not present in the ground-state calculations. Apart from this, the PN-RQRPA introduced in this work is self-consistent, i.e., the same interactions, both in the particle-hole and particle-particle channels, are used in the RHB equation that determines the canonical quasiparticle basis, and in the PN-RQRPA. In both channels, the same strength parameters of the interactions are used in the RHB and RQRPA calculations.

Similarly to the previous implementations of the PN-RQRPA [6], the two-quasiparticle configuration space includes states with both nucleons in the discrete bound levels, states with one nucleon in the bound levels and one nucleon in the continuum, and also states with both nucleons in the continuum. The RQRPA configuration space also includes pair-configurations formed from the fully or partially occupied states of positive energy and the empty negative-energy states from the Dirac sea [6]. As pointed out in Ref. [6], the inclusion of configurations built from occupied positive-energy states and empty negative-energy states is essential for the consistency of the model, as well as to reproduce the model independent sum rules.

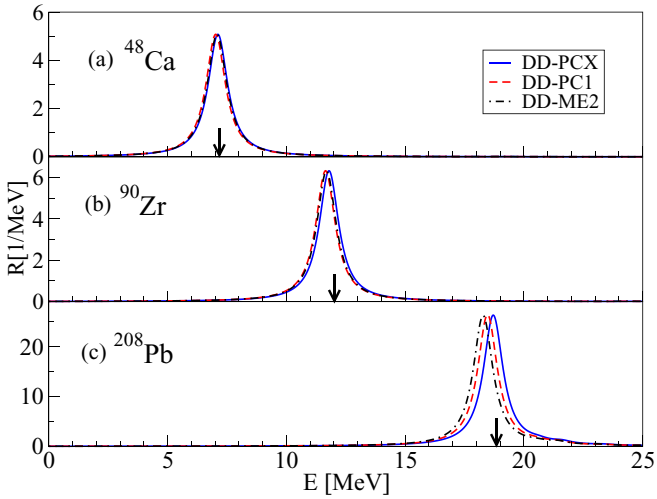

FIG. 1. The PN-RRPA isobaric analog resonance transition strength distribution for ^{48}Ca, ^{90}Zr, and ^{208}Pb, calculated using DD-PCX, DD-PC1, and DD-ME2 functionals.

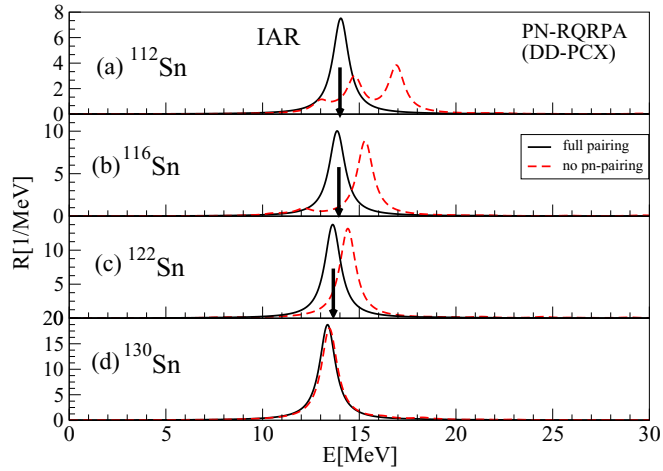

FIG. 2. The isobaric analog resonance transition strength distribution for ^{112,116,122,130}Sn, calculated with the PN-RQRPA using DD-PCX interaction. The results without (dashed line) and with (solid line) proton-neutron pairing in the residual PN-RQRPA interaction are shown separately, in comparison to the experimental data from Ref. [4], denoted by arrows.

Model calculations are based on 20 oscillator shells in the RHB model, as given as standard in Ref. [96] to achieve the convergence of the results. At the level of the PN-RQRPA calculations no truncations in the maximal excitation energy for the $2qp$ configuration space are used. We included a truncation of the $2qp$ configuration space by the condition on the corresponding occupation factors [6], $u_{qp1}v_{qp2} > 0.001$, in order to exclude $2qp$ configurations with two almost empty states. Further reducing of this limit value does not modify the results.

III. RESULTS

A. The isobaric analog resonance

The PN-R(Q)RPA based on point coupling interactions introduced in Sec. II is first implemented in the case of $J^\pi = 0^+$ charge-exchange transition, IAR. It is induced by the Fermi isospin-flip operator,

$$\hat{T}^F_{\beta^\pm} = \sum_{i=1}^{A} \tau_\pm. \tag{25}$$

Figure 1 shows the transition strength distributions for the IAR in closed-shell nuclei ^{48}Ca, ^{90}Zr and ^{208}Pb, calculated with the PN-RRPA using two density-dependent point coupling interactions, DD-PCX and DD-PC1, and density-dependent meson-exchange effective interaction DD-ME2. As expected, for each nucleus the response to the Fermi operator results in a pronounced single IAR peak. The IAR peak energy and transition strength display rather moderate model dependence. The most pronounced spread of the IAR excitation energies for different interactions, about 1 MeV, is obtained for the heaviest system, ^{208}Pb, while for ^{48}Ca and ^{90}Zr differences are smaller. The results of model calculations are compared with the experimental data for IAR excitation energies, denoted by arrows, obtained from (p, n) scattering on ^{48}Ca [104], ^{90}Zr [105,106], and ^{208}Pb [99]. Good agreement of the PN-RRPA results with the experimental data is obtained. In all three cases the calculated transition strengths of the IAR fulfill the Fermi nonenergy weighted sum rule, consistent with Ref. [6].

Next we explore the evolution of the IAR within the Sn isotope chain, for $A = 104$–132. In Fig. 2 the IAR transition strength distributions are shown for representative cases, ^{112,116,122,130}Sn. Model calculations are based on the PN-RQRPA with DD-PCX interaction. The results without and with the $T = 1$ proton-neutron pairing in the residual PN-RQRPA interaction are shown separately, in comparison to the experimental data from a systematic study of the (^{3}He, t) charge-exchange reaction in stable Sn isotopes [4]. As shown in Fig. 2, the full PN-RQRPA calculations result in a pronounced single IAR peak, with the excitation energy that is in excellent agreement with the experimental data for ^{112,116,122}Sn [4]. Complete treatment of paring correlations both in the RHB and PN-RQRPA is essential for description of the IAR [6]. This is illustrated in Fig. 2, where the strength functions are also shown without including the $T = 1$ proton-neutron residual pairing interaction, i.e., only the the ph-channel of the RQRPA residual interaction is included. Without the contributions of the pp channel, pronounced fragmentation of the transition strength is obtained for ^{112,116}Sn, and the excitation energies are overestimated. By including the attractive proton-neutron pairing interaction, the transition strength becomes redistributed toward a single pronounced IAR peak, that is consistent with the expectation of a narrow resonance peak from the experimental study [4]. More pronounced effect of the residual pairing interaction is obtained for ^{112,116,122}Sn, while for ^{130}Sn that is near the neutron closed shell the effect is rather small.

Figure 3 shows the evolution of the IAR excitation energy for the isotopic chain $^{104-132}$Sn, with the proton-neutron pairing included in the PN-RQRPA. The results are shown for

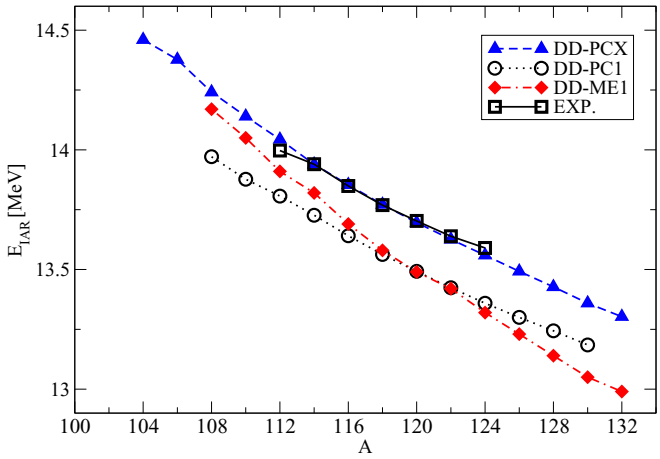

FIG. 3. The PN-RQRPA isobaric analog resonance excitation energy for the isotope chain $^{104-132}$Sn, with the proton-neutron pairing included. Calculations are based on the point coupling interaction DD-PCX and DD-PC1. The results from the previous study based on DD-ME1 interaction [6] and the experimental data from Ref. [4] are shown for comparison.

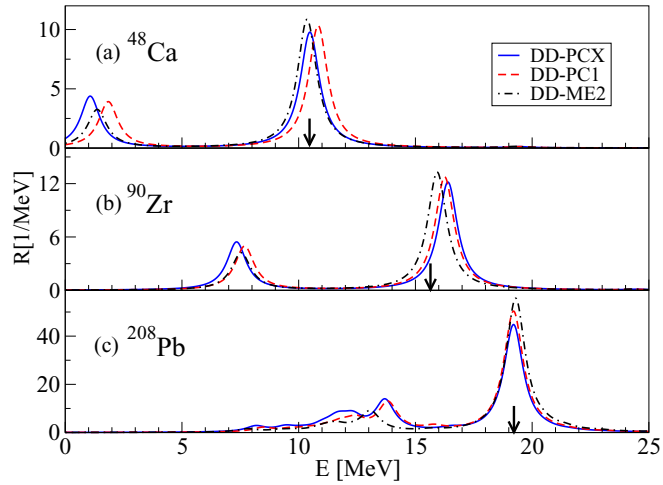

FIG. 4. The GT$^-$ strength distribution for ^{48}Ca, ^{90}Zr, and ^{208}Pb, calculated using the DD-PCX, DD-PC1, and DD-ME2 functionals. The experimental values of the main GT$^-$ peak for ^{48}Ca [104], ^{90}Zr [106], and ^{208}Pb [4,98,99] are denoted with arrows.

the point coupling interactions DD-PCX and DD-PC1. For comparison, the IAR excitation energies from the previous study based on DD-ME1 interaction [6] and the experimental data from Ref. [4] are displayed. As one can observe in the figure, recently established interaction DD-PCX reproduces the experimental data with high accuracy, while the DD-PC1 and DD-ME1 interactions provide systematically lower energies. We note that DD-PCX parametrization has been established using additional constraints on nuclear collective transitions that resulted with improved isovector properties, essential for the description of nuclear ground state, excitation phenomena, and nuclear matter properties around the saturation density [94]. Clearly, the PN-RQRPA framework based on DD-PCX interaction introduced in this work represents a considerable progress in comparison to other approaches.

B. The Gamow-Teller resonance

The Gamow-Teller transitions involve both the spin and isospin degrees of freedom. In the charge-exchange excitation spectra, these transitions mainly concentrate in a pronounced resonance peak—GTR, representing a coherent superposition of $J^\pi = 1^+$ proton-particle—neutron-hole transitions of neutrons from orbitals with $j = l + \frac{1}{2}$ into protons in orbitals with $j = l - \frac{1}{2}$. The GT transitions are excited by the spin-isospin operator

$$T^{\mathrm{GT}}_{\beta^\pm} = \sum_{i=1}^{A} \boldsymbol{\Sigma}\tau_\pm. \tag{26}$$

Figure 4 shows the GT$^-$ transition strength distribution for closed-shell nuclei ^{48}Ca, ^{90}Zr and ^{208}Pb, calculated with the PN-RQRPA using DD-PCX and DD-PC1 interactions. For comparison, the results of the meson exchange functional with the DD-ME2 parametrization are also shown. The experimental values for the main GT$^-$ peak are denoted with arrows for ^{48}Ca [104], ^{90}Zr [105,106], and ^{208}Pb [98–100]. Since the PN-RQRPA excitation energies are given with respect to the mother nucleus, the experimental values given with respect to daughter nucleus are obtained by adding the mass difference between the daughter and mother isotopes as well as the mass difference between neutron and proton which is missing when the GT is built on the basis of p-h excitations [67,107]. The transition strength distributions are dominated by the main Gamow-Teller resonance peak, that is composed from direct spin-flip transitions, ($j = l + \frac{1}{2} \rightarrow j = l - \frac{1}{2}$). In addition, pronounced low-energy GT$^-$ strength is obtained, composed from the core-polarization spin-flip ($j = l \pm \frac{1}{2} \rightarrow j = l \pm \frac{1}{2}$), and back spin-flip transitions ($j = l - \frac{1}{2} \rightarrow j = l + \frac{1}{2}$). As it is well known, quantitative description of the low-energy GT$^-$ strength is essential in modeling β decay half-lives [23,108]. When using three different effective interactions as shown in Fig. 4, the spread of values of the GT$^-$ excitation energies within ≈1 MeV is obtained.

While the strength parameter of the pseudovector channel in the residual PN-R(Q)RPA interactions is constrained by the GTR excitation energy in ^{208}Pb, reasonable agreement with experimental data is obtained for ^{48}Ca and ^{90}Zr without additional adjustments of the effective interaction. As it has already been discussed in previous studies, the Ikeda sum rule for GT transition strength [56] is fully reproduced in a complete calculation that includes both the configurations formed from occupied states in the Fermi sea and empty negative-energy states in the Dirac sea [6,109–112]. Table I shows the summary of the GTR properties for ^{48}Ca, ^{90}Zr, and ^{208}Pb for DD-PCX and DD-PC1 interactions: centroid excitation energies, the total transition strength difference $\sum B(\mathrm{GT}^-) - B(\mathrm{GT}^+)$ in comparison to the Ikeda sum rule [56] (in %), contributions of the Dirac sea states to the sum rule (in %), and the respective experimental values [99,104–106,113]. While the calculations accurately exhaust the Ikeda sum rule values, obtained total transition strengths in ^{48}Ca and ^{90}Zr for

TABLE I. Calculated and experimental GT^- properties, strength contributions for both GT^- and GT^+ channel, i.e., $\sum B(GT^-)$ and $\sum B(GT^+)$, and total transition strengths $\sum B(GT^-) - B(GT^+)$ for ^{48}Ca, ^{90}Zr, and ^{208}Pb, for DD-PCX and DD-PC1 interactions. The total transition strengths are given in percentages of the Ikeda sum rule value $3(N-Z)$ [56], and contributions from the negative energy states of the Dirac sea are shown. The experimental values for ^{48}Ca are from Refs. [104,113], ^{90}Zr from Refs. [105,106,114,115], and ^{208}Pb from Refs. [99,100].

		^{48}Ca	^{90}Zr	^{208}Pb
Experiment	E_1 (E_x) (MeV)	8.3 (≈10.5 [104])	15.5	19.2
	FWHM_1	1.5	3.8	4.1
	E_2 (MeV)	10.9	—	—
	FWHM_2	3.9	—	—
	$\sum B(GT^- + IVSM^-)$	15.3 ± 2.2 [113]	34.2 ± 1.6 [106]	—
	$\sum B(GT^-)$	—	28.0 ± 1.6 [106]	—
	$\sum B(GT^+ + IVSM^+)$	2.8 ± 0.3 [113]	—	—
	$\sum B(GT^+)$	1.9 ± 0.5 [113]	1.0 ± 0.3 [114] \$1.7 ± 0.2)[115]	—
	$3(N-Z)$	24	30	132
	$\sum B(GT^-) - B(GT^+)$ (%)	(52 ± 9)% \$≈70% [104])	(90 ± 5)% [106]	60–70% [99]
DD-PCX	E_x (MeV)	10.61	16.73	19.21
	$\sum B(GT^-)$	27.34	38.99	147.33
	$\sum B(GT^+)$	3.34	8.89	15.33
	$\sum B(GT^-) - B(GT^+)$ (%)	99.96%	100.33%	99.99%
	Dirac sea (%)	6.48%	7.90%	8.23%
DD-PC1	E_x (MeV)	10.98	16.54	19.21
	$\sum B(GT^-)$	27.09	37.21	145.92
	$\sum B(GT^+)$	3.10	7.05	13.93
	$\sum B(GT^-) - B(GT^+)$ (%)	99.97%	100.50%	99.99%
	Dirac sea (%)	5.93%	7.46%	7.48%

GT^- channel are somewhat larger than experimental ones for both point coupling interactions. After subtraction of the estimated IVSM contribution (usually ∼10%) the values of total GT^- strengths are even lower [113]. In the GT^+ channel for ^{48}Ca the difference between theoretical and experimental values is reduced, i.e., $\sum B(GT^+) = 3.3$ (3.0) for DD-PCX (DD-PC1) and it is very close to the experimental value of $\sum B(GT^+ + IVSM^-) = 2.8$ [$\sum B(GT^+) = 1.9$ without IVSM]. However, the experimental strengths in ^{48}Ca may be significantly underestimated for higher excitation energies above 15 MeV in the GT^- spectrum and above 8 MeV in the GT^+ spectrum [113]. The largest discrepancy in the GT^+ channel is observed for ^{90}Zr, where calculated values are at least few times greater than the highest estimates of experimental GT^+ strengths [115]. Other nonrelativistic RPA approaches, such as Extended RPA theories account also somewhat larger value of $\sum B(GT^-)$ (usually 10–20%) in lower part of ^{48}Ca excitation spectrum ($E_x \lesssim 20$ MeV) [116]. Both dressed and extended RPA theories overestimate total experimental strengths in ^{90}Zr for GT^- channel by 20–60% for $E_x \lesssim 25$ MeV. However, in these calculations significant percentage of the sum rule for both GT^- and GT^+ may be found for excitation energies above $E_x \gtrsim 40$ MeV [116], which is not the case in our calculations. The nonrelativistic QRPA + PVC calculations also overestimate the total experimental strengths in ^{48}Ca (71% of the RPA+PVC strength) and ^{208}Pb (63% of the RPA+PVC strength) [117], still not providing the explanation for the missing experimental strength. The contributions of the GT transitions to the empty Dirac sea in doubly magic nuclei is from 6.5 to 8.2% (5.9 to 7.5%) of the total strength for DD-PCX (DD-PC1), in agreement with the previous studies [6]. In the following, the PN-RQRPA based on point coupling interaction DD-PCX is employed in the study of GT^- transitions in Sn istotope chain. For open shell nuclei, in addition to the separable pairing interaction included in the RHB, the PN-RQRPA residual interaction also includes the isoscalar proton-neutron pairing as introduced in Sec. II. Since this pairing interaction channel is not present within the RHB, its strength parameter V_0 can be constrained by the experimental data, e.g., on GT^- excitation energies or β decay half-lives. Rather than providing the optimal value of V_0, in the present analysis we explore the pairing properties and sensitivity of the GT^- transitions by systematically varying V_0. In Fig. 5, the GT^- strength distribution is shown for the isotopes ^{112,116,122,130}Sn, calculated with the PN-RQRPA using DD-PCX interaction. The isoscalar proton-neutron pairing interaction strength parameter is varied within the range of $V_0 = 0$–1.3 MeV. At higher excitation energies, a pronounced GT resonance peak is obtained, except for ^{122}Sn, where the main peak is split. In all cases, pronounced low-energy GT^- strength is obtained, spreading over the energy range of ≈5 MeV. While the direct spin-flip transitions ($\nu j = l + \frac{1}{2} \rightarrow \pi j = l - \frac{1}{2}$) dominate the high-energy region, the low-energy strength is dominated by core-polarization spin-flip ($\nu j = l \pm \frac{1}{2} \rightarrow \pi j = l \pm \frac{1}{2}$), and back spin-flip ($\nu j = l - \frac{1}{2} \rightarrow \pi j = l + \frac{1}{2}$) transitions. Considering the dependence of the GT^- strength on the $T = 0$ proton-neutron pairing, one can observe in Fig. 5 that the main GTR peak appears insensitive

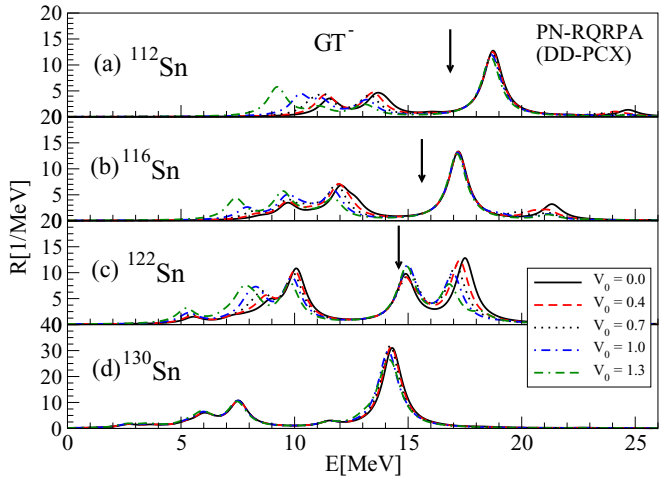

FIG. 5. The GT$^-$ strength distribution for ^{112,116,122,130}Sn, calculated with the PN-RQRPA using DD-PCX interaction, for the range of values of the isoscalar proton-neutron pairing interaction strength parameter, $V_0 = 0$–1.3. Experimental values for the main GT$^-$ peaks for ^{112}Sn, ^{116}Sn, and ^{122}Sn are denoted with arrows [4].

to this pairing interaction channel. In the low-energy region, pronounced sensitivity of the GT$^-$ spectra on V_0 is obtained, i.e., with increased V_0 the strength is shifted toward lower energies. This result is in agreement with previous studies based on different effective interactions both in the *ph* and *pp* channels [6].

In Table II the calculated GT strengths for the ^{112,116,122,130}Sn isotopes are shown for DD-PCX and DD-PC1 functionals, using $T = 0$ strength parameter set to $V_0 = 0.7$ and $V_0 = 1.3$. The Ikeda sum rule [56] is reasonably well reproduced.

In Table III calculated values of moments m_0(GT$^-$) are shown for the first three dominant GT$^-$ peaks, with the corresponding excitation energies m_1/m_0 with respect to the IAS for ^{112}Sn, ^{116}Sn, ^{122}Sn, and ^{130}Sn. Calculations include the DD-PCX functional and $T = 0$ pairing strength $V_0 = 1.3$. We note that there are few methods one can use to constrain the value of parameter V_0. One of them is based on comparison of experimental and theoretical values of relative positions of the GT peaks with respect to the IAS. As shown in Fig. 5, the number, position and intensity of GT peaks strongly depend on the value of parameter V_0. In the GTR spectrum of Sn isotopes one can observe two less intense distinguishable peaks for $V_0 \lesssim 0.4$ in the lower part of spectrum (GT2 and (GT3), besides one (GT1) or two dominant peaks (GT1a and GT1b), which is characteristic for $A \gtrsim 122$. For values $V_0 \gtrsim 0.4$ usually the third peak (GT4) starts to show up, while for values $V_0 \gtrsim 0.7$ we have in general three smaller peaks in lower part of spectrum that may be distinguished. The position of these peaks and respective transition strengths are strongly influenced by $T = 0$ pairing, i.e., with higher strength V_0 their positions move toward lower energies. Furthermore, the strength distribution is also modified, i.e., GT3 and GT4 peaks become more dominant than the GT2 ones for values $V_0 \gtrsim 1.3$. The influence of $T = 0$ pairing becomes suppressed when approaching the magic neutron number $N = 82$, as observed in the GTR spectrum of ^{130}Sn. Experimental values of GT positions and cross sections obtained from Sn(^{3}He, t)Sb reactions (see Ref. [4]) have some hierarchy, with descending values of cross sections corresponding to each peak as the peak position is moved toward lower energies, with minor

TABLE II. Calculated values of GTR properties for ^{112}Sn, ^{116}Sn, ^{122}Sn, and ^{130}Sn with DD-PCX and DD-PC1 interactions and $T = 0$ pairing strengths $V_0 = 0.7$ and $V_0 = 1.3$. The contributions of strengths in the GT$^-$ and GT$^+$ channels are shown in separate columns. The total strength of GTR is also represented in percentages of the Ikeda sum rule value, $3(N - Z)$ [56]. Contributions to total GTR strength from transitions to negative energy states of Dirac sea are also shown.

						Sum rule (%)	
		$3(N-Z)$	$\sum B(\mathrm{GT}^-)$	$\sum B(\mathrm{GT}^+)$	$\sum[B(\mathrm{GT}^-) - B(\mathrm{GT}^+)]$	Total	Dirac sea
DD-PCX	^{112}Sn	36	47.22	11.68	35.53	98.69%	7.36%
($V_0 = 0.7$)	^{116}Sn	48	57.77	9.99	47.77	99.53%	7.84%
	^{122}Sn	66	75.26	9.34	65.91	99.87%	7.87%
	^{130}Sn	90	99.06	9.12	89.94	99.94%	7.76%
DD-PC1	^{112}Sn	36	45.55	9.84	35.71	99.21%	7.11%
($V_0 = 0.7$)	^{116}Sn	48	57.03	9.26	47.77	99.53%	7.85%
	^{122}Sn	66	74.41	8.47	65.94	99.91%	7.17%
	^{130}Sn	90	98.23	8.26	89.96	99.96%	7.01%
DD-PCX	^{112}Sn	36	45.68	10.15	35.52	98.69%	7.36%
($V_0 = 1.3$)	^{116}Sn	48	56.79	7.59	49.20	99.53%	7.85%
	^{122}Sn	66	74.96	9.04	65.91	99.87%	7.87%
	^{130}Sn	90	99.01	9.06	89.94	99.94%	7.76%
DD-PC1	^{112}Sn	36	44.67	8.95	35.71	99.21%	7.12%
($V_0 = 1.3$)	^{116}Sn	48	56.29	8.46	47.82	99.64%	7.20%
	^{122}Sn	66	74.26	8.32	65.94	99.91%	7.18%
	^{130}Sn	90	98.20	8.23	89.96	99.96%	7.02%

TABLE III. Calculated values of moments m_0 and corresponding energy m_1/m_0 with respect to the IAS for the first four dominant GT$^-$ peaks for ^{112}Sn, ^{116}Sn, ^{122}Sn, and ^{130}Sn. The DD-PCX functional and $T = 0$ pairing strengths $V_0 = 0.7$ and $V_0 = 1.3$ are used. The experimental results for the difference between GTR and IAS, i.e., $\Delta^{\rm exp} = E^{\rm exp}_{\rm GTR} - E^{\rm exp}_{\rm IAS}$ and differential cross sections $d\sigma/d\Omega$ are taken from Ref. [4]. † For ^{122}Sn, the moments m_0 and m_1/m_0 contain contributions from two most dominant peaks.

				$V_0 = 0.7$			$V_0 = 1.3$		
		$\Delta^{\rm exp}$ (MeV)	$d\sigma/d\Omega$ (mb/sr)	m_0	m_1/m_0 (MeV)	$(\frac{m_1}{m_0} - E^{\rm teo}_{\rm IAS})$ (MeV)	m_0	m_1/m_0 (MeV)	$(\frac{m_1}{m_0} - E^{\rm teo}_{\rm IAS})$ (MeV)
GT1	^{112}Sn	2.78	12.4	19.11	18.70	4.85	17.69	18.63	4.78
	^{116}Sn	1.68	16.8	20.51	17.19	3.45	19.71	17.15	3.41
	^{122}Sn†	1.01	21.9	31.68	16.71	3.14	29.62	15.82	2.25
	^{130}Sn	—	—	50.03	14.22	0.83	48.55	14.12	0.73
GT2	^{112}Sn	−2.08	4.9	6.30	13.27	−0.58	3.69	13.05	−0.80
	^{116}Sn	−3.32	6.2	10.02	11.85	−1.89	6.54	11.61	−2.13
	^{122}Sn	−4.59	9.2	14.26	9.94	−3.63	11.27	9.78	−3.79
	^{130}Sn	—	—	15.75	7.53	−5.86	16.07	7.40	−5.99
GT3	^{112}Sn	−3.67	1.5	5.17	11.31	−2.54	2.54	11.06	−2.79
	^{116}Sn	−5.18	2.1	3.04	10.64	−3.10	8.71	9.52	−4.22
	^{122}Sn	−7.87	6.3	10.27	8.33	−5.24	12.81	7.87	−5.70
	^{130}Sn	—	—	9.74	5.87	−7.52	10.90	5.80	−7.59
GT4	^{112}Sn	−4.83	2.0	3.14	10.71	−3.14	8.94	9.01	−4.84
	^{116}Sn	−6.52	2.5	2.05	8.12	−5.62	6.65	7.33	−6.41
	^{122}Sn	−9.79	1.2	3.32	5.86	−7.71	5.64	5.59	−7.98

exception of GT4 which intensity is similar to the GT3 one or somewhat larger. Therefore we may impose some constraints on the value of V_0, which should be at least ≈0.7 in order to reproduce the GTR properties observed in experiments.

In Fig. 6 the PN-RQRPA results for the GT$^-$ direct spin-flip transition excitation energy centroid with the respect to the IAR energy are shown for the chain of even-even isotopes $^{104-132}$Sn. The available experimental data obtained from Sn(^{3}He, t)Sb charge-exchange reactions are shown for comparison [4]. The PN-RQRPA calculations are performed for the range of values of the isoscalar proton-neutron pairing interaction strength parameter, $V_0 = 0.4$–2.5. The point coupling interaction DD-PCX is used and the results based on the DD-ME2 interaction are also displayed [6]. We noticed almost linear decrease of differences between the GTR and IAS energies in Sn isotope chain as function of A or N (while keeping $Z = 50$ fixed). Similar observations may be found in nonrelativistic calculations with Skyrme parametrizations in Reference [118]. One can observe that the proton-neutron pairing interaction systematically reduces the GT-IAR energy splittings along the Sn isotope chain, resulting in good agreement for $V_0 \approx 2.5$. We note that relatively higher values of V_0 are required to reproduce the GT-IAR energy splittings. In Refs. [6,119], it has been emphasized that the energy difference between the GTR and the IAS reflects the magnitude of the effective spin-orbit potential. As one can see in Fig. 6, the GT-IAR energy splittings reduce in neutron-rich Sn isotopes toward zero value, reflecting considerable reduction of the spin-orbit potential and the corresponding increase of the neutron skin thickness $r_n - r_p$ [119]. Therefore, as pointed out in Ref. [119], the energy difference $E_{\rm GT} - E_{\rm IAS}$, obtained from the experiment, could be used to determine the value of neutron skin thickness in a consistent framework that can simultaneously describe the charge-exchange excitation properties and the $r_n - r_p$ value, such as the RHB+PN-RQRPA approach.

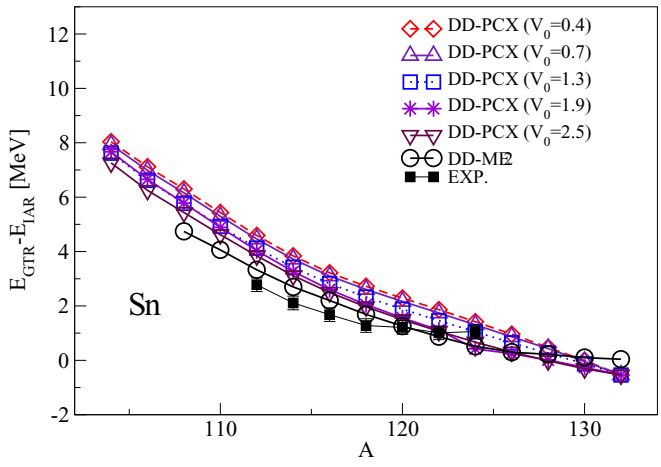

FIG. 6. The PN-RQRPA excitation energy for GT$^-$ direct spin-flip transitions for $^{104-132}$Sn, for the range of values of the isoscalar proton-neutron pairing interaction strength parameter V_0. Calculations are based on the density-dependent point coupling interaction DD-PCX and the results from the previous study based on the DD-ME2 interaction [6] and the experimental data from Ref. [4] are shown for comparison.

In Ref. [107] the GT$^-$ transition strength for ^{118}Sn was analyzed in more details, including the finite temperature effects, using the Skyrme functional SkM*. In the present study, for ^{118}Sn without $T = 0$ pairing and DD-PCX interaction ($V_0 = 0$), we obtain pronounced low-lying GT$^-$ states at energies $E = 7.32$, 8.88, 9.64, 10.21, and 11.45 MeV with

the corresponding transition strengths $B(\mathrm{GT}^-) = 1.21$, 3.25, 1.12, 1.14, and 14.30. The main GTR peaks are obtained at $E = 16.46$ and 19.83 MeV with $B(\mathrm{GT}^-) = 19.91$ and 7.69, respectively. The excitation energies are comparable with the respective values obtained for the SkM* interaction in Ref. [107], $E(\mathrm{GT}^-) = 6.2$, 8.9, 10.5, 16.3 and 20.2 MeV [107]. Study in Ref. [107] also showed that relativistic calculations of GT^- transitions in ^{118}Sn with density-dependent meson-exchange interaction DD-ME2 lead to the splitting between major (GT1a) and energetically higher somewhat less intensive peak (GT1b), that exists only for $V_0 \lesssim 200$ MeV in $T = 0$ pairing channel. For $V_0 \approx 200$ MeV the two peaks start to merge, while for $V_0 \gtrsim 240$ MeV they are completely replaced by one somewhat stronger peak shifted ≈0.5 MeV toward higher energies. However, nonrelativistic calculations in Refs. [107,118] show different behavior in GT^- spectrum of ^{118}Sn with respect to $T = 0$ pairing strength, i.e., the two dominant peaks never merge, even for large values of overall strength of the $T = 0$ pairing (≈800 MeV). The same feature is obtained in the present study, as shown in Fig. 5 for ^{122}Sn. We note that relativistic calculation in Ref. [107] used another pairing interaction in $T = 0$ channel than the nonrelativistic one, i.e., two Gaussians with different relative strengths to cover short and medium distances in coordinate space introduced separately for the PN-RQRPA. This caused additional interplay between attractive and repulsive terms which act differently for the short and medium ranges. Therefore, behavior of the GTR spectrum obtained in our study is more similar to the nonrelativistic calculations in Refs. [107,118], where the zero range density-dependent surface pairing in both isospin channels is introduced separately in the PN-RQRPA.

IV. CONCLUSION

In this work we have formulated a consistent framework for description of nuclear charge-exchange transitions based on the proton-neutron relativistic quasiparticle random phase approximation in the canonical single-nucleon basis of the relativistic Hartree-Bogoliubov model, using density-dependent relativistic point coupling interactions. The implementation of recently established DD-PCX interaction [94], adjusted not only to the nuclear ground state properties, but also with the symmetry energy of the nuclear equation of state and the incompressibility of nuclear matter constrained using collective excitation data, allows improved description of ground-state and excitation properties of nuclei far from stability, that is important for the studies of exotic nuclear structure and dynamics, as well as for applications in nuclear astrophysics. The introduced formalism based on point coupling interactions is also relevant from the practical point of view, because it allows efficient systematic large-scale calculations of nuclear properties and processes of relevance for the nucleosynthesis and stellar evolution modeling. In the current formulation of the RHB+PN-RQRPA, the pairing correlations are implemented by the separable pairing force [95] that allows accurate and efficient calculations of the pairing properties. The PN-RQRPA includes both the $T = 1$ and $T = 0$ pairing channels. While the $T = 1$ channel corresponds to the pairing interaction constrained at the ground-state level, $T = 0$ proton-neutron pairing strength parameter can be determined from the experimental data on charge-exchange transitions and β decay half lives. In order to validate the PN-R(Q)RPA framework introduced in this work, spin and isospin excitations—isobaric analog resonances and Gamow-Teller transitions—have been investigated in several closed-shell nuclei and Sn isotope chain. The results show very good agreement with the experimental data, representing an improvement compared to previous studies based on the relativistic nuclear energy density functionals. When compared to other theoretical approaches that usually underestimate the IAR excitation energies in Sn isotope chain, the present model using DD-PCX interaction accurately reproduces the experimental data. Therefore, the framework introduced in this work represents an important contribution for the future studies of astrophysically relevant nuclear excitations and weak interaction processes, in particular β decay in neutron-rich nuclei, electron capture in presupernova stage of massive stars, and neutrino-nucleus reactions relevant for the synthesis of elements in the universe and stellar evolution. Especially important is the extension of theory framework introduced in this work to include both the finite temperature effects together with nuclear pairing and apply it for the description of electron capture and β decay at finite temperature characteristic for stellar environment [107,120]. This work is currently in progress [26,44].

ACKNOWLEDGMENTS

Stimulating discussions with Ante Ravlić are gratefully acknowledged. This work is supported by the QuantiXLie Centre of Excellence, a project co financed by the Croatian Government and European Union through the European Regional Development Fund, the Competitiveness and Cohesion Operational Programme (KK.01.1.1.01). Y.F.N. acknowledges support from the National Natural Science Foundation of China under Grant No. 12075104.

APPENDIX A: PARTICLE-HOLE MATRIX ELEMENTS

For the isovector-pseudovector part of particle-hole channel in the PN-RQRPA we use the contact type of interaction with constant coupling,

$$V_{\mathrm{PV}} = -\alpha_{\mathrm{PV}}[\gamma_5\,\gamma^{\nu}\vec{\tau}]_1\,[\gamma_5\gamma_{\nu}\vec{\tau}]_2\,\delta(\vec{r}_1 - \vec{r}_2). \tag{A1}$$

The uncoupled matrix element of isovector-pseudovector interaction is given by

$$\langle a\,b|V|c\,d\rangle = -\alpha_{\mathrm{PV}}\int dr r^2 \sum_{L\lambda}\left[\int dr_1 r_1^2 \int d\Omega_1 \bar{\psi}_a(r_1,\Omega_1)[\gamma_5\,\gamma^{\nu}\vec{\tau}]_{(1)}Y^*_{L\lambda}(\Omega_1)\delta(r-r_1)\psi_c(r_1,\Omega_1)\right]$$

$$\times \left[\int dr_2 r_2^2 \int d\Omega_2 \bar{\psi}_b(r_2, \Omega_2)[\gamma_5\ \gamma_\nu \vec{\tau}]_{(2)} Y_{L\lambda}(\Omega_2)\ \delta(r - r_2)\ \psi_d(r_2, \Omega_2) \right], \tag{A2}$$

where we used expansion of delta function in spherical coordinates [121],

$$\delta(\vec{r}_1 - \vec{r}_2) = \frac{\delta(r_1 - r_2)}{r_1 r_2} \sum_{\lambda\mu} Y^*_{\lambda\mu}(\Omega_1) Y_{\lambda\mu}(\Omega_2), \tag{A3}$$

$$= \int dr r^2 \frac{\delta(r - r_1)\delta(r - r_2)}{r^2 r_1 r_2} \sum_{\lambda\mu} Y^*_{\lambda\mu}(\Omega_1) Y_{\lambda\mu}(\Omega_2). \tag{A4}$$

Indices a, b, c, and d refer to all quantum numbers involved, while the Dirac's conjugate is defined in standard way as

$$\bar{\psi}_a = \psi_a^+\ \gamma_0. \tag{A5}$$

If we ignore for a moment the isospin part of the wave function (corresponding quantum numbers isospin t and its third projection t_0) one can rewrite Eq. (A2) in the following form:

$$\langle am_a\ bm_b|V|cm_c\ dm_d\rangle^{\rm PV} = -\alpha_{\rm PV} \int dr r^2 \sum_{\lambda\mu} (-1)^\mu \sum_\nu \left[Q^\nu_{\lambda\mu}(r, \Omega_1)\right]_{ac} [Q_{\lambda-\mu;\nu}(r, \Omega_2)]_{bd}, \tag{A6}$$

where the index ν refers to Dirac matrix γ_ν (γ^ν) in the vertex and we used (see Ref. [97] for the sherical case of spinor):

$$\left[Q^\nu_{\lambda\mu}(r, \Omega_i)\right]_{am_a\ cm_c} = \int d\Omega_i [f_{n_a\kappa_a}(r)\Omega^\dagger_{\kappa_a m_a}(\Omega_i) \ - ig_{n_a\kappa_a}(r)\Omega^\dagger_{\bar{\kappa}_a m_a}(\Omega_i)][\gamma_0\gamma_5\ \gamma^\nu]_{(i)} Y_{\lambda\mu}(\Omega_i) \begin{bmatrix} f_{n_c\kappa_c}(r)\Omega_{\kappa_a m_c}(\Omega_i) \\ ig_{n_c\kappa_c}(r)\Omega_{\bar{\kappa}_c m_c}(\Omega_i) \end{bmatrix}, \tag{A7}$$

where the subscripts 1 and 2 refer to $\Omega_{i=1,2} = (\theta_i, \phi_i)$, while radial parts of bispinors $f(r)$ and $g(r)$ are assumed to be real in our case. From Eq. (A7) one can easily obtain timelike

$$\begin{aligned} \left[Q^0_{\lambda\mu}(r, \Omega_i)\right]_{am_a\ cm_c} = &- [i\ f_{n_a\kappa_a}(r)\ g_{n_c\kappa_c}(r)\langle(1/2\ l_a)j_a m_a|\ Y_{\lambda\mu}(\Omega_i)|(1/2\bar{l}_c)j_c m_c\rangle \\ &- i\ g_{n_a\kappa_a}(r)\ f_{n_c\kappa_c}(r)\langle(1/2\bar{l}_a)j_a m_a|\ Y_{\lambda\mu}(\Omega_i)|(1/2 l_c)j_c m_c\rangle] \end{aligned} \tag{A8}$$

and spacelike components ($k = 1$, 2, and 3)

$$\begin{aligned} \left[Q^k_{\lambda\mu}(r, \Omega_i)\right]_{am_a\ cm_c} = &- [f_{n_a\kappa_a}(r) f_{n_c\kappa_c}(r)\langle(1/2 l_a)j_a m_a|\sigma_k Y_{\lambda\mu}(\Omega_1)|(1/2 l_c)j_c m_c\rangle \\ &+ g_{n_a\kappa_a}(r) g_{n_c\kappa_c}(r)\langle(1/2\bar{l}_a)j_a m_a|\sigma_k Y_{\lambda\mu}(\Omega_1)|(1/2\bar{l}_c)j_c m_c\rangle]. \end{aligned} \tag{A9}$$

In order to couple particle and hole operator, i.e., states, into good total angular momentum J (and projection M) in the matrix elements of the residual particle-hole two body interaction, one needs to start from [122]

$$|(ph^{-1})JM\rangle = [c^\dagger_p h^\dagger_h]_{JM}|0\rangle, \tag{A10}$$

$$= \sum_{m_p m_h} C^{JM}_{j_p m_p j_h m_h} c^\dagger_{pm_p} h^\dagger_{hm_h}|0\rangle, \tag{A11}$$

$$= \sum_{m_p m_h} (-1)^{j_h - m_h} C^{JM}_{j_p m_p j_h - m_h} a^\dagger_{pm_p} a_{h\ m_h}|0\rangle, \tag{A12}$$

from which JJ-coupled particle-hole matrix element follows directly

$$\langle ac^{-1}|V|b^{-1}d\rangle^{JM} = \sum_{m_a m_c} (-1)^{j_c - m_c} C^{J\ M}_{j_a\ m_a\ j_c\ -m_c} \sum_{m_b m_d} (-1)^{j_b - m_b} C^{J\ M}_{j_d\ m_d\ j_b\ -m_b} \langle am_a\ bm_b|V|cm_c\ dm_d\rangle. \tag{A13}$$

Using the Wigner-Eckart theorem for angular parts in Eqs. (A8) and (A9) after some manipulations with Clebsch-Gordan coefficients one obtains the ph matrix elements in JJ-coupled form. Therefore, after including isospin part of the matrix elements, which gives a factor of 2, which we have ignored for the moment, for the timelike part of pseudovector coupling we obtain:

$$\begin{aligned} V^{({\rm PVt})J}_{abcd} = &\frac{2\alpha_{\rm PV}}{2J+1} \langle(1/2 l_a)j_a||Y_J(\Omega_1)||(1/2\bar{l}_c)j_c\rangle\langle(1/2 l_d)j_d||Y_J(\Omega_2)||(1/2\bar{l}_b)j_b\rangle \\ &\times \int dr r^2 [f_a(r)g_c(r) - g_a(r)f_c(r)][f_b(r)g_d(r) - g_b(r)f_d(r)] \end{aligned} \tag{A14}$$

and for spacelike part

$$V^{({\rm PVs})J}_{abcd} = \frac{2\alpha_{\rm PV}}{2J+1} \sum_L \int dr r^2 [f_a(r)f_c(r)\langle(1/2\ l_a)j_a||[\sigma_S Y_L]_J||(1/2\ l_c)j_c\rangle + g_a(r)g_c(r)\langle(1/2\ \bar{l}_a)j_a||[\sigma_S Y_L]_J||(1/2\ \bar{l}_c)j_c\rangle]$$

$$\times [f_b(r)f_d(r)\langle(1/2\ l_d)j_d||[\sigma_S Y_L]_J||(1/2\ l_b)j_b\rangle + g_b(r)g_d(r)\langle(1/2\ \bar{l}_d)j_d||[\sigma_S Y_L]_J||(1/2\ \bar{l}_b)j_b\rangle], \tag{A15}$$

where the reducible angular part of matrix elements can be written in terms of 3jm symbols:

$$\langle(1/2l_a)j_a||Y_J||(1/2l_c)j_c\rangle = \frac{1+(-1)^{l_a+l_c+J}}{2}\frac{\hat{j}_a\hat{j}_c\hat{J}}{\sqrt{4\pi}}(-1)^{j_a-1/2}\begin{pmatrix} j_a & J & j_c \\ -1/2 & 0 & 1/2\end{pmatrix}, \tag{A16}$$

and

$$\langle(1/2l_a)j_a||[\sigma_S Y_L]_J||(1/2l_c)j_c\rangle = \frac{1+(-1)^{l_a+l_c+J}}{2}\frac{\hat{j}_a\hat{j}_c\hat{J}\hat{L}}{\sqrt{4\pi}}(-1)^{l_a+L} \times\left[(-1)^{l_c+j_c+1/2}\begin{pmatrix}1 & L & J\\ 0 & 0 & 0\end{pmatrix}\begin{pmatrix} j_a & J & j_c \\ -1/2 & 0 & 1/2\end{pmatrix} - \sqrt{2}\begin{pmatrix}1 & L & J\\ -1 & 0 & 1\end{pmatrix}\begin{pmatrix} j_a & J & j_c \\ 1/2 & -1 & 1/2\end{pmatrix}\right]. \tag{A17}$$

Note that the timelike pseudovector matrix elements are nonzero only in the case of unnatural parity transitions, like Gamow-Teller transition. The isovector-vector part of two-body interaction is given by

$$V_V = \alpha_V[\rho_V(r_1)][\gamma^\mu\vec{\tau}]_1\ [\gamma_\mu\vec{\tau}]_2\ \delta(\vec{r}_1-\vec{r}_2). \tag{A18}$$

There are no additional rearrangement terms due to isospin restriction of the PN-R(Q)RPA, i.e., changing the nucleon from neutron to proton or vice versa and properties of the point coupling functional itself. Therefore, one should start from Eq. (A18) and follow the same procedure described before, from Eqs. (A2) to (A15), replacing Eqs. (A8) and (A9) with

$$\begin{aligned}\left[Q^k_{\lambda\mu}(r,\Omega_i)\right]_{am_a\ cm_c} = [&if_{n_a\kappa_a}(r)g_{n_c\kappa_c}(r)\langle(1/2\ l_a)j_a m_a|\sigma_k Y_{\lambda\mu}(\Omega_i)|(1/2\ \bar{l}_c)j_c m_c\rangle \\ &- ig_{n_a\kappa_a}(r)f_{n_c\kappa_c}(r)\langle(1/2\ \bar{l}_a)j_a m_a|\sigma_k Y_{\lambda\mu}(\Omega_i)|(1/2l_c)j_c m_c\rangle]\end{aligned} \tag{A19}$$

and

$$\begin{aligned}\left[Q^0_{\lambda\mu}(r,\Omega_i)\right]_{am_a\ cm_c} = [&f_{n_a\kappa_a}(r)f_{n_c\kappa_c}(r)\langle(1/2\ l_a)j_a m_a|Y_{\lambda\mu}(\Omega_i)|(1/2\ l_c)j_c m_c\rangle \\ &+ g_{n_a\kappa_a}(r)g_{n_c\kappa_c}(r)\langle(1/2\ \bar{l}_a)j_a m_a|Y_{\lambda\mu}(\Omega_i)|(1/2\ \bar{l}_c)j_c m_c\rangle]\end{aligned} \tag{A20}$$

in order to obtain JJ-coupled ph matrix elements for this channel, i.e., spacelike part

$$\begin{aligned}V^{(\mathrm{TVs})J}_{abcd} = \frac{2}{2J+1}\sum_L\int drr^2\alpha_{\mathrm{TV}}[\rho_V(r)][&f_a(r)g_c(r)\langle(1/2\ l_a)j_a||[\sigma_S Y_L]_J||(1/2\ \bar{l}_c)j_c\rangle \\ &- g_a(r)f_c(r)\langle(1/2\ \bar{l}_a)j_a||[\sigma_S Y_L]_J||(1/2\ l_c)j_c\rangle][f_b(r)g_d(r)\langle(1/2\ \bar{l}_d)||[\sigma_S Y_L]_J||(1/2\ l_b)j_b\rangle \\ &- g_b(r)f_d(r)\langle(1/2\ l_d)j_d||[\sigma_S Y_L]_J||(1/2\ \bar{l}_b)j_b\rangle]\end{aligned} \tag{A21}$$

and timelike part

$$\begin{aligned}V^{(\mathrm{TVt})J}_{abcd} = \frac{2}{2J+1}\int drr^2\alpha_{\mathrm{TV}}[\rho_V(r)][&f_a(r)f_c(r)+g_a(r)g_c(r))][f_b(r)f_d(r)+g_b(r)g_d(r)] \\ &\times\langle(1/2\ l_a)j_a||Y_J||(1/2\ l_c)j_c\rangle\langle(1/2\ l_d)j_d||Y_J||(1/2\ l_b)j_b\rangle.\end{aligned} \tag{A22}$$

APPENDIX B: NATURAL EXTENSION OF SEPARABLE PAIRING

In order to extend the standard $S=0$ ($T=1$) pairing, which was used in the RHB and RQRPA, one needs to start from general expression for particle-particle matrix element in the uncoupled form:

$$V_{abcd} = \langle n_a(1/2l_a)j_a\ n_b(1/2l_b)j_b|V(1-\hat{P}^r\hat{P}^\sigma\hat{P}^\tau)|n_c(1/2l_c)j_c\ n_d(1/2l_d)j_d\rangle, \tag{B1}$$

where $\hat{P}^r$, $\hat{P}^\sigma$, and $\hat{P}^\tau$ represent the exchange of relative spatial coordinate, spin and isospin, respectively. For action of the spin exchange operator $\hat{P}^\sigma$ we simply have

$$P^\sigma\,|(1/2_{(1)}1/2_{(2)})SM_S\rangle = (-1)^{S+1}\,|(1/2_{(1)}1/2_{(2)})SM_S\rangle, \tag{B2}$$

which affects just the order of coupling, i.e., the phase $(-1)^{S+1}$ of symmetry transformation of the Clebsch-Gordan coefficient. Furthermore, one may construct P^σ mathematically in the following way:

$$\hat{P}_\sigma = \frac{1+\vec{\sigma}_1\cdot\vec{\sigma}_2}{2}, \tag{B3}$$

and isospin exchange operator in analogous way. However, the action of $\hat{P}^r$ affects only relative spatial coordinates,

$$\hat{P}^r|NLM_L\rangle = |NLM_L\rangle, \tag{B4}$$

$$\hat{P}^r|nlm_l\rangle = (-1)^l|nlm_l\rangle, \tag{B5}$$

Therefore, as first step one needs to do the *LS* recoupling in *bra* and *ket* independently

$$\begin{aligned} V^{(\text{pair})J}_{abcd} = {} & \hat{j}_a\hat{j}_b\hat{j}_c\hat{j}_d \sum_{\lambda S}\sum_{\lambda' S'} \hat{\lambda}\hat{S}\hat{\lambda}'\hat{S}' \begin{Bmatrix} s_a & l_a & j_a \\ s_b & l_b & j_b \\ S & \lambda & J \end{Bmatrix} \begin{Bmatrix} s_c & l_c & j_c \\ s_d & l_d & j_d \\ S' & \lambda' & J \end{Bmatrix} \sum_{TM_T}\sum_{T'M_{T'}} C^{TM_T}_{1/2-1/21/21/2} C^{T'M_{T'}}_{1/2-1/21/21/2} \\ & \times \sum_{M_S M'_S} C^{JM}_{SM_S\lambda\mu} C^{JM}_{S'M'_S\lambda'\mu'} \langle (1/2\ 1/2)TM_T|\langle (s_a s_b)SM_S(l_a l_b)\lambda\mu|V(1-\hat{P}^r\hat{P}^\sigma\hat{P}^\tau) \\ & \times |(s_c s_d)S'M'_S(l_c l_d)\lambda'\mu'\rangle|(1/2\ 1/2)T'M_{T'}\rangle. \end{aligned} \tag{B6}$$

In the second step one needs to substitute V with generic separable form, similarly to Eq. (17) but now without any kind of projection,

$$V(\vec{r}_1,\vec{r}_2,\vec{r}'_1,\vec{r}'_2) = -G_0\delta(\vec{R}_1-\vec{R}_2)G(r)G(r') \tag{B7}$$

into Eq. (B6) and transform the laboratory coordinates $\vec{r}_1$ and $\vec{r}_2$ ($\vec{r}'_1$ and $\vec{r}'_2$) in *bra* (*ket*) into the center of mass $\vec{R}$ ($\vec{R}'$) and relative coordinates $\vec{r}$ ($\vec{r}'$), i.e., the so-called Talmi-Moschinsky transformation. Therefore we need to evaluate

$$\begin{aligned} & \sum_{TM_T}\sum_{T'M_{T'}} C^{TM_T}_{1/2-1/21/21/2} C^{T'M_{T'}}_{1/2-1/21/21/2} \langle (1/2\ 1/2)TM_T|\langle (1/2\ 1/2)SM_S(l_a l_b)\lambda\mu| \\ & V(1-\hat{P}^r\hat{P}^\sigma\hat{P}^\tau)|(1/2\ 1/2)S'M_{S'}(l_c l_d)\lambda'\mu'\rangle|(1/2\ 1/2)T'M_{T'}\rangle \\ & = -4\pi G_0\delta_{SS'}\delta_{M_S M_{S'}}\delta_{\lambda L}\delta_{\mu m_L}\delta_{\lambda' L}\delta_{\mu' m_{L'}} \sum_{NLnn'} I_n I_{n'} M^{NLn0}_{n_a l_a n_b l_b} M^{NLn'0}_{n_c l_c n_d l_d} \sum_T \frac{1}{2}[1+(-1)^{S'+T+1}]. \end{aligned} \tag{B8}$$

Constraining ourself to the proton-neutron case only, note that the only nonvanishing cases of the isospin coupling are $T=0$ and $M_T=0$ or $T=1$ and $M_T=0$, which both lead to factor $1/2$ in front of the round brackets in Eq. (B6). Therefore, substituting back Eq. (B8) into Eq. (B6) after some mathematical manipulations we obtain

$$V^{JM}_{abcd} = -G_0\hat{j}_a\hat{j}_b\hat{j}_c\hat{j}_d \sum_{LS}\sum_T \frac{1}{2}[1+(-1)^{S'+T+1}]\tilde{f}(S,T)\hat{S}^2\hat{L}^2 \begin{Bmatrix} l_b & 1/2 & j_b \\ l_a & 1/2 & j_a \\ L & S & J \end{Bmatrix} \begin{Bmatrix} l_d & 1/2 & j_d \\ l_c & 1/2 & j_c \\ L & S & J \end{Bmatrix} \sum_{nn'} \tilde{I}_n\tilde{I}'_n M^{NLn0}_{n_a l_a n_b l_b} M^{NLn'0}_{n_c l_c n_d l_d}. \tag{B9}$$

However, we also add multiplication with function $\tilde{f}(S,T)$ which should take into account somewhat smaller or enhanced effect of the pairing in $T=0$ case,

$$\tilde{f}(S,T) = \begin{cases} 1, & \text{for } S=0,\ T=1 \\ V_{0pp}, & \text{for } S=1,\ T=0 \\ 0, & \text{the rest} \end{cases} \tag{B10}$$

while $\tilde{I}_n = \sqrt{4\pi}I_n$ is spatial integral of Gaussian $G(r)$ derived analytically in the next section of Appendix.

APPENDIX C: ANALYTICAL SOLUTION OF RADIAL PART

Radial part of the eigenfunction of spherical three-dimensional harmonic oscillator is given by

$$R_{nl}(r,b_0) = b_0^{-3/2}R_{nl}(\xi^2) = b_0^{-3/2}N_{nl}\xi^l L_n^{l+1/2}(\xi^2)e^{-\xi^2/2}, \tag{C1}$$

where b_0 represents oscillatory length, while n corresponds to the nodes number (in this notation we do not take into account 0 and ∞). Possible values are $n=0,1,2,\ldots$, and $\xi = r/b_0$.

Normalization factor N_{nl} is given by

$$N_{nl} = \left[\frac{2n!}{\Gamma(l+n+3/2)}\right]^{1/2}. \tag{C2}$$

In the case of half-number arguments gamma function is given by

$$\Gamma\left(\frac{1}{2}+n\right) = \frac{1\cdot 3\cdot 5\cdots(2n-1)}{2^n}\sqrt{\pi} = \frac{(2n-1)!!}{2^n}\sqrt{\pi}, \tag{C3}$$

We are interested in the analytical solution of the following integral

$$I_n = \int R_{nl}(r)G(r)r^2 dr. \tag{C4}$$

By inserting G(r) from Eq. (18) in Eq. (C4) we obtain

$$I_n = \frac{b_0^{3/2}N_{n0}}{(4\pi a^2)^{3/2}} \int_0^\infty \exp\left[-\frac{\xi^2}{2}\left(\frac{b_0^2}{a^2}+1\right)\right] L_n^{1/2}(\xi^2)\xi^2 d\xi. \tag{C5}$$

After substitution

$$\alpha^2 = \frac{a^2}{b_0^2}, \quad \xi^2 = \eta \rightarrow \xi d\xi = \frac{d\eta}{2}, \tag{C6}$$

Eq. (C5) can be rewritten as

$$I_n = \frac{b_0^{-3/2}N_{n0}}{(4\pi\alpha^2)^{3/2}} \frac{1}{2} \int_0^\infty \exp\left[-\eta + \frac{\eta}{2}\left(1-\frac{1}{\alpha^2}\right)\right] \times L_n^{(1/2)}(\eta)\sqrt{\eta} d\eta. \tag{C7}$$

Generating function for Laguerre polynomials with $\alpha = 1/2$ ($l = 0$) is given by expression [123]

$$\frac{1}{(1-z)^{3/2}} \exp\left(\frac{xz}{z-1}\right) = \sum_{n=0}^\infty L_n^{1/2}(x) z^n. \tag{C8}$$

By using substitution

$$\frac{1}{2}\left(1-\frac{1}{\alpha^2}\right) = \frac{z}{z-1} \rightarrow z = \frac{1-\alpha^2}{1+\alpha^2} \tag{C9}$$

and Eq. (C8), we can rewrite Eq. (C7) in the following form,

$$I_n = \frac{b_0^{-3/2}N_{n0}}{(4\pi\alpha^2)^{3/2}} \frac{1}{2}(1-z)^{3/2} \sum_{m=0}^\infty z^m \int_0^\infty \times d\eta \eta^{1/2} e^{-\eta} L_n^{(1/2)}(\eta) L_m^{(1/2)}(\eta). \tag{C10}$$

The integral in Eq. (C10) is just orthogonality condition for Laguerre's polynomials [123],

$$\int_0^\infty x^\alpha e^{-\alpha} L_n^\alpha(x) L_m^\alpha(x) dx = \frac{\Gamma(n+\alpha+1)}{n!}\delta_{nm}. \tag{C11}$$

Therefore, Eq. (C10) reduces to

$$I_n = \frac{1}{2}\frac{b_0^{-3/2}N_{n0}}{(4\pi\alpha^2)^{3/2}}(1-z)^{3/2} \sum_{m=0}^\infty z^m \frac{\Gamma(m+3/2)}{m!}\delta_{nm}. \tag{C12}$$

Using Eq. (C3), inserting normalization factor [Eq. (C2)] and expressing everything in terms of α and n, after some mathematical manipulations, it can further be simplified to

$$I_n = \frac{1}{2^{5/2}\pi^{5/4}b_0^{3/2}} \frac{(1-\alpha^2)^n}{(1+\alpha^2)^{n+3/2}} \frac{\sqrt{(2n+1)!}}{2^n n!}. \tag{C13}$$

[1] N. Auerbach, J. Hüfner, A. K. Kerman, and C. M. Shakin, Rev. Mod. Phys. **44**, 48 (1972).
[2] N. Auerbach, Phys. Rep. **98**, 273 (1983).
[3] O. A. Rumyantsev and M. H. Urin, Phys. Rev. C **49**, 537 (1994).
[4] K. Pham, J. Jänecke, D. A. Roberts, M. N. Harakeh, G. P. A. Berg, S. Chang, J. Liu, E. J. Stephenson, B. F. Davis, H. Akimune, and M. Fujiwara, Phys. Rev. C **51**, 526 (1995).
[5] G. Colò, H. Sagawa, N. Van Giai, P. F. Bortignon, and T. Suzuki, Phys. Rev. C **57**, 3049 (1998).
[6] N. Paar, T. Nikšić, D. Vretenar, and P. Ring, Phys. Rev. C **69**, 054303 (2004).
[7] S. Fracasso and G. Colò, Phys. Rev. C **72**, 064310 (2005).
[8] X. Roca-Maza, G. Colò, and H. Sagawa, Phys. Rev. C **86**, 031306(R) (2012).
[9] X. Roca-Maza and N. Paar, Prog. Part. Nucl. Phys. **101**, 96 (2018).
[10] M. Bender, J. Dobaczewski, J. Engel, and W. Nazarewicz, Phys. Rev. C **65**, 054322 (2002).
[11] T. Marketin, G. Martínez-Pinedo, N. Paar, and D. Vretenar, Phys. Rev. C **85**, 054313 (2012).
[12] E. Litvinova, B. A. Brown, D. L. Fang, T. Marketin, and R. G. T. Zegers, Phys. Lett. B **730**, 307 (2014).
[13] A. Ekström, G. R. Jansen, K. A. Wendt, G. Hagen, T. Papenbrock, S. Bacca, B. Carlsson, and D. Gazit, Phys. Rev. Lett. **113**, 262504 (2014).
[14] V. Zelevinsky, N. Auerbach, and B. M. Loc, Phys. Rev. C **96**, 044319 (2017).
[15] H. Morita and Y. Kanada-En'yo, Phys. Rev. C **96**, 044318 (2017).
[16] J.-U. Nabi, M. Ishfaq, M. Böyükata, and M. Riaz, Nucl. Phys. A **966**, 1 (2017).
[17] E. Ha and M.-K. Cheoun, Eur. Phys. J. A **53**, 26 (2017).
[18] J. Engel, P. Vogel, and M. R. Zirnbauer, Phys. Rev. C **37**, 731 (1988).
[19] I. Borzov, S. Fayans, and E. Trykov, Nucl. Phys. A **584**, 335 (1995).
[20] J. Engel, M. Bender, J. Dobaczewski, W. Nazarewicz, and R. Surman, Phys. Rev. C **60**, 014302 (1999).
[21] I. N. Borzov, Phys. Rev. C **67**, 025802 (2003).
[22] M. Madurga, S. V. Paulauskas, R. Grzywacz, D. Miller, D. W. Bardayan, J. C. Batchelder, N. T. Brewer, J. A. Cizewski, A. Fijałkowska, C. J. Gross, M. E. Howard, S. V. Ilyushkin, B. Manning, M. Matoš, A. J. Mendez, K. Miernik, S. W. Padgett, W. A. Peters, B. C. Rasco, A. Ratkiewicz, K. P. Rykaczewski, D. W. Stracener, E. H. Wang, M. Wolinska-Cichocka, and E. F. Zganjar, Phys. Rev. Lett. **117**, 092502 (2016).
[23] T. Marketin, L. Huther, and G. Martínez-Pinedo, Phys. Rev. C **93**, 025805 (2016).
[24] B. Moon, C.-B. Moon, A. Odahara, R. Lozeva, P.-A. Söderström, F. Browne, C. Yuan, A. Yagi, B. Hong, H. S. Jung, P. Lee, C. S. Lee, S. Nishimura, P. Doornenbal, G. Lorusso, T. Sumikama, H. Watanabe, I. Kojouharov, T. Isobe, H. Baba *et al.*, Phys. Rev. C **96**, 014325 (2017).
[25] Z. Y. Wang, Y. F. Niu, Z. M. Niu, and J. Y. Guo, J. Phys. G: Nucl. Part. Phys. **43**, 045108 (2016).
[26] A. Ravlić, E. Yüksel, Y. F. Niu, and N. Paar, arXiv:2010.06394.
[27] R. Caballero-Folch, C. Domingo-Pardo, J. Agramunt, A. Algora, F. Ameil, A. Arcones, Y. Ayyad, J. Benlliure, I. N.

Borzov, M. Bowry, F. Calviño, D. Cano-Ott, G. Cortés, T. Davinson, I. Dillmann, A. Estrade, A. Evdokimov, T. Faestermann, F. Farinon, D. Galaviz *et al.*, Phys. Rev. Lett. **117**, 012501 (2016).
[28] A. Faessler and F. Simkovic, J. Phys. G: Nucl. Part. Phys. **24**, 2139 (1998).
[29] J. Suhonen and O. Civitarese, Phys. Rep. **300**, 123 (1998).
[30] F. Šimkovic, R. Hodák, A. Faessler, and P. Vogel, Phys. Rev. C **83**, 015502 (2011).
[31] J. Menéndez, D. Gazit, and A. Schwenk, Phys. Rev. Lett. **107**, 062501 (2011).
[32] J. D. Vergados, H. Ejiri, and F. Šimkovic, Rep. Prog. Phys. **75**, 106301 (2012).
[33] J. Menéndez, T. R. Rodríguez, G. Martínez-Pinedo, and A. Poves, Phys. Rev. C **90**, 024311 (2014).
[34] D. c. v. Štefánik, F. Šimkovic, and A. Faessler, Phys. Rev. C **91**, 064311 (2015).
[35] D. Navas-Nicolás and P. Sarriguren, Phys. Rev. C **91**, 024317 (2015).
[36] D. S. Delion and J. Suhonen, Phys. Rev. C **95**, 034330 (2017).
[37] K. Langanke and G. Martinez-Pinedo, Nucl. Phys. A **673**, 481 (2000).
[38] K. Langanke and G. Martínez-Pinedo, Rev. Mod. Phys. **75**, 819 (2003).
[39] H. T. Janka, K. Langanke, A. Marek, G. Martínez-Pinedo, and B. Müller, The Hans Bethe Centennial Volume 1906-2006, Phys. Rep. **442**, 38 (2007).
[40] S. Noji, R. G. T. Zegers, S. M. Austin, T. Baugher, D. Bazin, B. A. Brown, C. M. Campbell, A. L. Cole, H. J. Doster, A. Gade, C. J. Guess, S. Gupta, G. W. Hitt, C. Langer, S. Lipschutz, E. Lunderberg, R. Meharchand, Z. Meisel, G. Perdikakis, J. Pereira *et al.*, Phys. Rev. Lett. **112**, 252501 (2014).
[41] N. Paar, T. Marketin, D. Vale, and D. Vretenar, Int. J. Mod. Phys. E **24**, 1541004 (2015).
[42] Y. F. Niu, N. Paar, D. Vretenar, and J. Meng, Phys. Rev. C **83**, 045807 (2011).
[43] Z. M. Niu, Y. F. Niu, Q. Liu, H. Z. Liang, and J. Y. Guo, Phys. Rev. C **87**, 051303(R) (2013).
[44] A. Ravlić, E. Yüksel, Y. F. Niu, G. Colò, E. Khan, and N. Paar, Phys. Rev. C **102**, 065804 (2020).
[45] M. Arnould, S. Goriely, and K. Takahashi, Phys. Rep. **450**, 97 (2007).
[46] K. Mori, M. A. Famiano, T. Kajino, T. Suzuki, J. Hidaka, M. Honma, K. Iwamoto, K. Nomoto, and T. Otsuka, Astrophys. J. **833**, 179 (2016).
[47] H. Ejiri, Phys. Rep. **338**, 265 (2000).
[48] T. Suzuki and H. Sagawa, Nucl. Phys. A **718**, 446 (2003).
[49] D. Frekers, H. Ejiri, H. Akimune, T. Adachi, B. Bilgier, B. A. Brown, B. T. Cleveland, H. Fujita, Y. Fujita, M. Fujiwara, E. Ganioğlu, V. N. Gavrin, E. W. Grewe, C. J. Guess, M. N. Harakeh, K. Hatanaka, R. Hodak, M. Holl, C. Iwamoto, N. T. Khai *et al.*, Phys. Lett. B **706**, 134 (2011).
[50] M.-K. Cheoun, E. Ha, S. Y. Lee, K. S. Kim, W. Y. So, and T. Kajino, Phys. Rev. C **81**, 028501 (2010).
[51] N. Paar, D. Vretenar, T. Marketin, and P. Ring, Phys. Rev. C **77**, 024608 (2008).
[52] N. Paar, T. Suzuki, M. Honma, T. Marketin, and D. Vretenar, Phys. Rev. C **84**, 047305 (2011).
[53] M. Karakoç, R. G. T. Zegers, B. A. Brown, Y. Fujita, T. Adachi, I. Boztosun, H. Fujita, M. Csatlós, J. M. Deaven, C. J. Guess, J. Gulyás, K. Hatanaka, K. Hirota, D. Ishikawa, A. Krasznahorkay, H. Matsubara, R. Meharchand, F. Molina, H. Okamura, H. J. Ong *et al.*, Phys. Rev. C **89**, 064313 (2014).
[54] F. Osterfeld, Rev. Mod. Phys. **64**, 491 (1992).
[55] Y. Fujita, B. Rubio, and W. Gelletly, Prog. Part. Nucl. Phys. **66**, 549 (2011).
[56] K. Ikeda, S. Fujii, and J. I. Fujita, Phys. Lett. **3**, 271 (1963).
[57] R. R. Doering, A. Galonsky, D. M. Patterson, and G. F. Bertsch, Phys. Rev. Lett. **35**, 1691 (1975).
[58] J. A. Halbleib and R. A. Sorensen, Nucl. Phys. A **98**, 542 (1967).
[59] I. S. Towner and F. C. Khanna, Phys. Rev. Lett. **42**, 51 (1979).
[60] C. D. Goodman, C. A. Goulding, M. B. Greenfield, J. Rapaport, D. E. Bainum, C. C. Foster, W. G. Love, and F. Petrovich, Phys. Rev. Lett. **44**, 1755 (1980).
[61] G. Brown and M. Rho, Nucl. Phys. A **372**, 397 (1981).
[62] G. F. Bertsch and I. Hamamoto, Phys. Rev. C **26**, 1323 (1982).
[63] K. Nakayama, A. Pio Galeão, and F. Krmpotić, Phys. Lett. B **114**, 217 (1982).
[64] N. Van Giai and H. Sagawa, Phys. Lett. B **106**, 379 (1981).
[65] C. Gaarde, Nucl. Phys. A **396**, 127 (1983).
[66] V. A. Kuzmin and V. G. Soloviev, J. Phys. G **10**, 1507 (1984).
[67] G. Colò, N. Van Giai, P. F. Bortignon, and R. A. Broglia, Phys. Rev. C **50**, 1496 (1994).
[68] I. Hamamoto and H. Sagawa, Phys. Rev. C **48**, R960 (1993).
[69] B. A. Brown and K. Rykaczewski, Phys. Rev. C **50**, R2270 (1994).
[70] T. Suzuki and T. Otsuka, Phys. Rev. C **56**, 847 (1997).
[71] C. De Conti, A. Galeão, and F. Krmpotić, Phys. Lett. B **444**, 14 (1998).
[72] E. Caurier, K. Langanke, G. Martínez-Pinedo, and F. Nowacki, Nucl. Phys. A **653**, 439 (1999).
[73] K. Langanke, E. Kolbe, and D. J. Dean, Phys. Rev. C **63**, 032801(R) (2001).
[74] A. Algora, B. Rubio, D. Cano-Ott, J. L. Taín, A. Gadea, J. Agramunt, M. Gierlik, M. Karny, Z. Janas, A. Płochocki, K. Rykaczewski, J. Szerypo, R. Collatz, J. Gerl, M. Górska, H. Grawe, M. Hellström, Z. Hu, R. Kirchner, M. Rejmund, E. Roeckl, M. Shibata, L. Batist, and J. Blomqvist (GSI Euroball Collaboration), Phys. Rev. C **68**, 034301 (2003).
[75] Y. Kalmykov, T. Adachi, G. P. A. Berg, H. Fujita, K. Fujita, Y. Fujita, K. Hatanaka, J. Kamiya, K. Nakanishi, P. von Neumann-Cosel, V. Y. Ponomarev, A. Richter, N. Sakamoto, Y. Sakemi, A. Shevchenko, Y. Shimbara, Y. Shimizu, F. D. Smit, T. Wakasa, J. Wambach *et al.*, Phys. Rev. Lett. **96**, 012502 (2006).
[76] C. L. Bai, H. Sagawa, H. Q. Zhang, X. Z. Zhang, G. Colò, and F. R. Xu, Phys. Lett. B **675**, 28 (2009).
[77] Y. S. Lutostansky, Phys. At. Nucl. **74**, 1176 (2011).
[78] M. Sasano, G. Perdikakis, R. G. T. Zegers, S. M. Austin, D. Bazin, B. A. Brown, C. Caesar, A. L. Cole, J. M. Deaven, N. Ferrante, C. J. Guess, G. W. Hitt, R. Meharchand, F. Montes, J. Palardy, A. Prinke, L. A. Riley, H. Sakai, M. Scott, A. Stolz *et al.*, Phys. Rev. Lett. **107**, 202501 (2011).
[79] Y. F. Niu, G. Colò, M. Brenna, P. F. Bortignon, and J. Meng, Phys. Rev. C **85**, 034314 (2012).
[80] E. Ha and M.-K. Cheoun, Phys. Rev. C **88**, 017603 (2013).
[81] X. Roca-Maza, G. Colò, and H. Sagawa, Phys. Scr. **2013**, 014011 (2013).
[82] M. Martini, S. Péru, and S. Goriely, Phys. Rev. C **89**, 044306 (2014).

[83] E. Ha and M.-K. Cheoun, Phys. Rev. C **94**, 054320 (2016).

[84] Y. F. Niu, G. Colò, E. Vigezzi, C. L. Bai, and H. Sagawa, Phys. Rev. C **94**, 064328 (2016).

[85] H. Z. Liang, H. Sagawa, M. Sasano, T. Suzuki, and M. Honma, Phys. Rev. C **98**, 014311 (2018).

[86] J. Yasuda, M. Sasano, R. G. T. Zegers, H. Baba, D. Bazin, W. Chao, M. Dozono, N. Fukuda, N. Inabe, T. Isobe, G. Jhang, D. Kameda, M. Kaneko, K. Kisamori, M. Kobayashi, N. Kobayashi, T. Kobayashi, S. Koyama, Y. Kondo, A. J. Krasznahorkay *et al.*, Phys. Rev. Lett. **121**, 132501 (2018).

[87] H. Liang, N. Van Giai, and J. Meng, Phys. Rev. Lett. **101**, 122502 (2008).

[88] Z. M. Niu, Y. F. Niu, H. Z. Liang, W. H. Long, and J. Meng, Phys. Rev. C **95**, 044301 (2017).

[89] P. Finelli, N. Kaiser, D. Vretenar, and W. Weise, Nucl. Phys. A **791**, 57 (2007).

[90] T. Marketin, E. Litvinova, D. Vretenar, and P. Ring, Phys. Lett. B **706**, 477 (2012).

[91] C. Robin and E. Litvinova, Phys. Rev. Lett. **123**, 202501 (2019).

[92] J. Dechargé and D. Gogny, Phys. Rev. C **21**, 1568 (1980).

[93] J. Berger, M. Girod, and D. Gogny, Comput. Phys. Commun. **63**, 365 (1991).

[94] E. Yüksel, T. Marketin, and N. Paar, Phys. Rev. C **99**, 034318 (2019).

[95] Y. Tian, Z.-Y. Ma, and P. Ring, Phys. Rev. C **79**, 064301 (2009).

[96] T. Nikšić, N. Paar, D. Vretenar, and P. Ring, Comput. Phys. Commun. **185**, 1808 (2014).

[97] W. Greiner and D. Bromley, *Relativistic Quantum Mechanics: Wave Equations* (Springer, Berlin, 2000).

[98] D. J. Horen, C. D. Goodman, C. C. Foster, C. A. Goulding, M. B. Greenfield, J. Rapaport, D. E. Bainum, E. Sugarbaker, T. G. Masterson, F. Petrovich, and W. G. Love, Phys. Lett. B **95**, 27 (1980).

[99] H. Akimune, I. Daito, Y. Fujita, M. Fujiwara, M. B. Greenfield, M. N. Harakeh, T. Inomata, J. Jänecke, K. Katori, S. Nakayama, H. Sakai, Y. Sakemi, M. Tanaka, and M. Yosoi, Phys. Rev. C **52**, 604 (1995).

[100] A. Krasznaborkay, H. Akimune, M. Fujiwara, M. N. Harakeh, J. Jänecke, V. A. Rodin, M. H. Urin, and M. Yosoi, Phys. Rev. C **64**, 067302 (2001).

[101] D. Vretenar, A. Afanasjev, G. Lalazissis, and P. Ring, Phys. Rep. **409**, 101 (2005).

[102] B. Buck and A. Merchant, Nucl. Phys. A **600**, 387 (1996).

[103] G. Kamuntavičius, R. Kalinauskas, B. Barrett, S. Mickevičius, and D. Germanas, Nucl. Phys. A **695**, 191 (2001).

[104] B. D. Anderson, T. Chittrakarn, A. R. Baldwin, C. Lebo, R. Madey, P. C. Tandy, J. W. Watson, B. A. Brown, and C. C. Foster, Phys. Rev. C **31**, 1161 (1985).

[105] D. E. Bainum, J. Rapaport, C. D. Goodman, D. J. Horen, C. C. Foster, M. B. Greenfield, and C. A. Goulding, Phys. Rev. Lett. **44**, 1751 (1980).

[106] T. Wakasa, H. Sakai, H. Okamura, H. Otsu, S. Fujita, S. Ishida, N. Sakamoto, T. Uesaka, Y. Satou, M. B. Greenfield, and K. Hatanaka, Phys. Rev. C **55**, 2909 (1997).

[107] E. Yüksel, N. Paar, G. Colò, E. Khan, and Y. F. Niu, Phys. Rev. C **101**, 044305 (2020).

[108] T. Marketin, D. Vretenar, and P. Ring, Phys. Rev. C **75**, 024304 (2007).

[109] H. Kurasawa, T. Suzuki, and N. Van Giai, Phys. Rev. Lett. **91**, 062501 (2003).

[110] H. Kurasawa, T. Suzuki, and N. Van Giai, Phys. Rev. C **68**, 064311 (2003).

[111] Z. Ma, B. Chen, and N. e. a. Van Giai, Eur. Phys. J. A **20**, 429 (2004).

[112] H. Kurasawa and T. Suzuki, Phys. Rev. C **69**, 014306 (2004).

[113] K. Yako, M. Sasano, K. Miki, H. Sakai, M. Dozono, D. Frekers, M. B. Greenfield, K. Hatanaka, E. Ihara, M. Kato, T. Kawabata, H. Kuboki, Y. Maeda, H. Matsubara, K. Muto, S. Noji, H. Okamura, T. H. Okabe, S. Sakaguchi, Y. Sakemi *et al.*, Phys. Rev. Lett. **103**, 012503 (2009).

[114] K. J. Raywood, B. M. Spicer, S. Yen, S. A. Long, M. A. Moinester, R. Abegg, W. P. Alford, A. Celler, T. E. Drake, D. Frekers, P. E. Green, O. Häusser, R. L. Helmer, R. S. Henderson, K. H. Hicks, K. P. Jackson, R. G. Jeppesen, J. D. King, N. S. P. King, C. A. Miller *et al.*, Phys. Rev. C **41**, 2836 (1990).

[115] H. Condé, N. Olsson, E. Ramström, T. Rönnqvist, R. Zorro, J. Blomgren, A. Håkansson, G. Tibell, O. Jonsson, L. Nilsson, P.-U. Renberg, M. Österlund, W. Unkelbach, J. Wambach, S. van der Werf, J. Ullmann, and S. Wender, Nucl. Phys. A **545**, 785 (1992).

[116] G. A. Rijsdijk, W. J. W. Geurts, M. G. E. Brand, K. Allaart, and W. H. Dickhoff, Phys. Rev. C **48**, 1752 (1993).

[117] Y. F. Niu, G. Colò, and E. Vigezzi, Phys. Rev. C **90**, 054328 (2014).

[118] S. Fracasso and G. Colò, Phys. Rev. C **76**, 044307 (2007).

[119] D. Vretenar, N. Paar, T. Nikšić, and P. Ring, Phys. Rev. Lett. **91**, 262502 (2003).

[120] E. Yüksel, G. Colò, E. Khan, Y. F. Niu, and K. Bozkurt, Phys. Rev. C **96**, 024303 (2017).

[121] P. Ring and P. Schuck, *The Nuclear Many-Body Problem*, Physics and Astronomy Online Library (Springer, Berlin, 2004).

[122] J. Suhonen, *From Nucleons to Nucleus: Concepts of Microscopic Nuclear Theory*, Theoretical and Mathematical Physics (Springer, Berlin, 2007).

[123] M. Abramowitz and I. Stegun, *Handbook of Mathematical Functions: With Formulas, Graphs, and Mathematical Tables*, Applied Mathematics Series (Dover, New York, 1965).